SST Mechanical Structure: Structural Analysis Report

SST-MEC-ANR-008

Version 2b

Prepared by:		
Gino Tosti (INAF)		SST-STR SE
Salvatore Scuderi (INAF)		SST-STR PM
Alessio Trois (INAF)		SST-STR PRM
Nicola La Palombara (INAF)		SST-PRO PRQM
Approved by:		
Gianpiero Tagliaferri		SST-ESC

Current Release				
Ver.	Created	Comment	Distribution	Editor(s)
2b	25/07/2023	Product Review RIX implemented	SST-PO	Gino Tosti

Version History				
Ver.	Created	Comment	Distribution	Editor(s)
1.aD1	03/11/2022	First draft issue	SST-PO	
1.aD2	29/11/2022	Added seismic bucking (4.5.3); comments to draft1 implemented	SST-PO	
2a	30/11/2022	Product Review issue	SST Team, CTAO, PR Board	

Table of Contents

List of Figures

List of Tables

1 Introduction

1.1 Scope & Purpose

This document is the SST Mechanical Structure Structural Analysis report.

It contains all the Finite Element modelling and analysis that has been performed on the SST structure of verify its structural integrity to the survival-level environmental actions and its performance and functionality to the operational loads.

In section 2 of the document, the assumptions of the performed analysis are explained.

In section 3, the FEM model of the telescope is described and validated via model checks.

In section 4, the analysis sequence is described, and the results presented.

Finally, in section 5, brief conclusions are drawn.

1.2 Applicable Documents

[AD1]	SST-PRO-PLA-001	SST Programme Management Plan
[AD2]	CTA-SPE-SEI-400000-0001-1c	CTAO South Seismic Risk Specification

1.3 Reference Documents

[RD1]	SST-MEC-DSR-001 2b	SST Mechanical Structure Design Report
[RD2]	SST-MEC-SPE-002 2b	SST Mechanical Structure Subsytem Specification
[RD3]	EN 1990	Eurocode 0 – basis of structural design
[RD4]	EN 1991	Eurocode 1 – actions on structures
[RD5]	EN 1993	Eurocode 3 – design of steel structures
[RD6]	EN 1998	Eurocode 8 – design of structures for earthquake resistance

1.4 Definition of Terms and Abbreviations

1.4.1 Abbreviations and Acronyms

AIT	Assembly Integration and Testing
AIV	Assembly Integration and Verification
ASTRI	Astrophysics with Italian Replicating Technology Mirrors
BKO	Bridging phase Kick-Off
BP	Bridging Phase
CDR	Critical Design Review
CoM	Center of Mass
CTA	Cherenkov Telescope Array
CTAO	Cherenkov Telescope Array Observatory
FAR	Final Acceptance Review
FRC	France Contribution
DR	Delivery Review
DVER	Design Verification Engineering Review
ERIC	European Research Infrastructure Consortium
ESC	Executive Steering Committee
FE	Finite Element
FEA	Finite Element Analysis
FEM	Finite Element Method
IKC	In Kind Contribution
INAF	Istituto Nazionale di Astrofisica
INSU	Institut National des Science de l'Univers
KO	Kick-Off
MPIK	Max-Planck-Institut für Kernphysik
OP	Observatoire de Paris – PSL, CNRS
PA	Product Assurance
PBS	Product Breakdown Structure
PM	Project Manager
PR	Product Review
PMP	Programme Management Plan
PO	Project Office
PRM	Programme Manager
PRR	Production Readiness Review
PSE	Programme System Engineer
QA	Quality Assurance
SE	System Engineer
SST	Small-Sized Telescope
TRR	Test Readiness Review
WBS	Work Breakdown Structure

1.4.2 Glossary

TERM	DEFINITION
"As Built" Configuration	The as-built configuration or applied configuration is defining the as-built status per each serial number of Configuration Item (CI) subject to formal acceptance.
"As Designed" Configuration	The as-designed configuration or Applicable configuration is defining the current design status of a Configuration Item (CI)
AIV	AIV is the Assembly Integration and Verification, which is referred to the integration activities related with the verification of the system or sub-system. In the framework of SST for briefness this term includes also the Assembly Integration and Testing which is related with the integration activities and testing to be performed during the integration at system and subsystem levels
Baseline	Set of information which describes exhaustively a situation at a given instant of time or over a given time interval.
Change	Vehicle for proposing modifications to an approved baselined data or the business agreement.
Configuration	Functional or physical Characteristics of a product defined in configuration definition documents subject to configuration baseline.
Configuration Item	Aggregation of hardware, software, processed materials, services or any of its discrete portions, that is designated for configuration management and treated as a single entity in the configuration management process. NOTE: A configuration item can contain other lower-level configuration item(s).
Deviation	Written authorization to depart from the originally specified requirements for a product prior to its production.
Firmware	Firmware is software programmed onto an electronic device which is treated like a pure hardware.
Executive Steering Committee	The SST Executive Steering Committee (ESC) is the high-level decision-making body which will manage the strategic direction of the Programme and will be in charge of overseeing progress and facilitating global collaboration among the participating groups.
Institutes	Research Institutes involved in the SST Programme.
Contractor	Industry involved in the SST Programme which has a contract whith an institute
SST-PRO	It is the team composed by Institutes and Contractors responsible , involved in the production of SST telescopes elements, which coordinate the project level activities.
Hardware	Hardware is a single or an assembly of physical electronic devices which cannot be changed in its user environment.
Item	Any part, component device, sub-unit, unit, equipment or device that can be individually considered.
Model	Physical or abstract representation of relevant aspects of an item or process that is put forward as a basis for calculations, predictions or further assessment useful for the preparation of SST production
Partners	are those entities taking responsibility for IKC delivery by signing IKC agreements with CTAO, plus any organisation identified by these signing entities as playing an essential role in SST delivery. The institutes are the partners of the CTA-SST consortium.
Product	A product (hardware, software, service) required in the frame of the program and included as element of the product tree having a unique identifier. A product may be deliverable or not.
Product Breakdown Structure	Hierarchical structure depicting the product orientated breakdown of the project into successive levels of detail down to the configuration items necessary to deliver the required functions. The Product Breakdown Structure (PBS) in general is influenced by Institutes/partners decisions to group certain products or by program history. It identifies products and their interfaces; it serves as the basis for the WBS
Service	Service is the result of at least one activity necessarily performed at the interface between the SST consortium and CTA and is generally intangible.
Software	Set of computer programs, procedures, documentation, and their associated data.
SST-E2E	The SST end-to-end telescope, or simply SST, will consist of the SST Structure and the SST Camera (including all mechanics, mirrors, auxiliary devices and required software), integrated and commissioned on-site including all required documents. It ends at (and integrates into CTA via) the system interfaces specified by the CTA PBS.
SST Consortium	The SST Consortium then consists of the Partners and their associated Teams, where a Team is a set of individuals within a single organisation at a single location (such as a University group).
System	An entity of products assembled or working together for a well defined specified purpose. In SST the term system can be utilised in alternative to Telescope End-to-End.
Sub-System	Like a system but a lower level. In SST the SST system is composed by the subsystem SST-MECH, SST-OPT, SST-TCS and SST-CAM.
Waiver	Written authorization to use or release a product which does not conform to the specified requirements
Work Breakdown Structure	Hierarchical representation of the activities necessary to complete a project.

2 Assumptions

The SST telescope Finite Element (FE) modelling and analysis have been performed adopting the following assumptions:

- All the performed analysis are linear elastic.
- All the defined material models are linear elastic.
- Mono-axial elements lie on the geometrical axis of the corresponding actual component.
- 2D elements lie on the mid plane of the corresponding actual component.
- 3D elements have the overall geometry of the corresponding actual component.
- The mass and the inertia of structural components are generally represented through their density. Contrarily, the mass of the non-structural components (e.g., instruments, cabinets, flanges, gratings, railings, motors, brakes…) is considered by means of concentrated mass elements.
- Non-structural components are either represented by concentrated or distributed mass elements. Concentrated mass elements are located in the object CoM and are connected to the relevant structural interfaces by means of contacts elements, which do not add stiffness to the model. Distributed mass elements are distributed as an added mass per unit length/surface.
- Optical components are modelled as concentrated mass elements, located in their respective CoM.
- Unless differently specified, all the actual joints are intended to restore the structure stiffness, so they have been represented with a continuous mesh. In particular, with reference to the steel structures, all the welded and bolted joints are represented as continuous.
  Environmental conditions for the different scenarios defined in the specifications are summarized here below:

	Favourable	Operational	Transition	Survival
Wind speed (10-min average)	11 km/h	36 km/h	50 km/h no damage 60 km/h within serviceability state	100 km/h
Wind speed (1-s gust)	-	-	-	170 km/h
Temperature Range	-	-5 °C / 25 °C	-	-15 °C / 35 °C

3 FE Model Description

3.1 FE Code

The analysis has been performed using ANSYS Workbench 18.2 software, importing the 3D modeled geometries into the finite element environment with the CAD software Autodesk INVENTOR.

The geometries modeled for the FEM analysis sometimes does not include all the details shown in the relative construction drawings.

It is good practice in the FEM analyses, in order to make the model lighter and obtain a regular mesh, to simplify the geometries in areas that are not of interest for the analysis, while maintaining all the details that are located in areas of interest or that have influence on the results, according to the experience of the structural analyst.

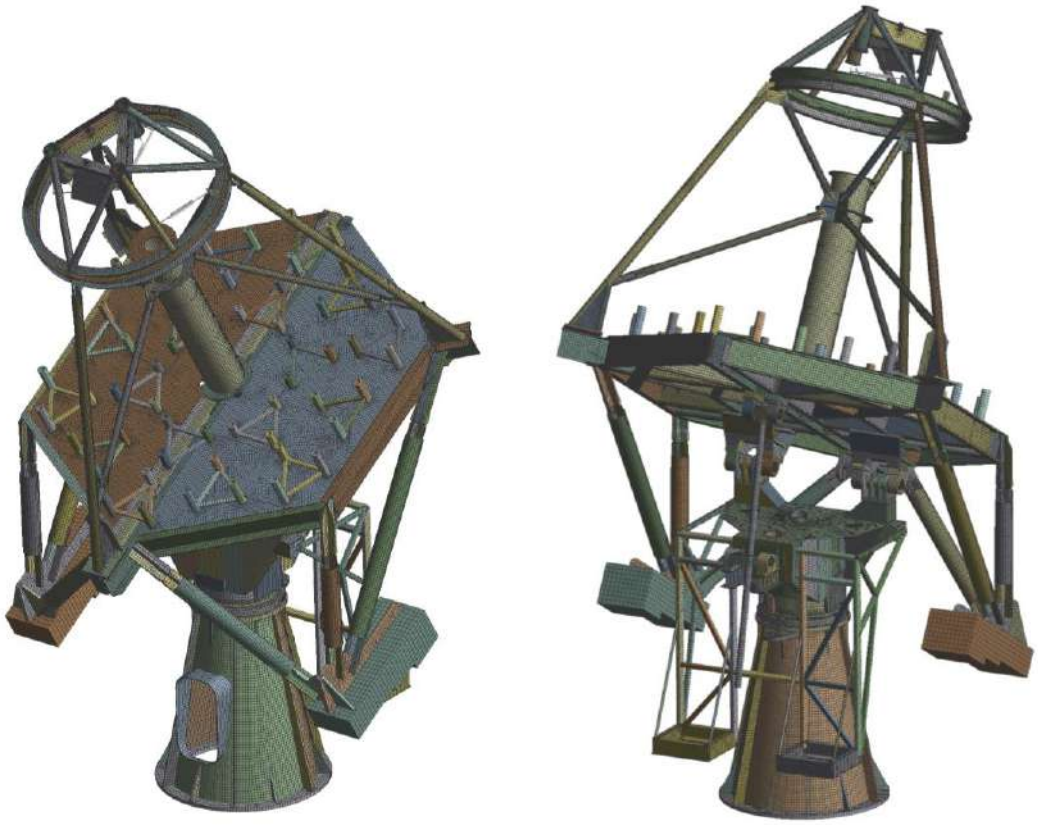

Figure 3-1: SST FEM model

3.2 Model Coordinate Systems

{XG, YG, ZG} is the Global Reference System. This reference system has the origin at the interface plane between the base of the telescope and the ground, has the Z axis emerging from the ground and aligned with the Azimuth axis, the X axis is parallel to the Elevation axis, and Y axis is oriented to respect the right-hand rule.

{XE, YE, ZE} is the Elevation reference System. This reference system has the X axis coincident with the elevation axis, Z axis aligned with the optical axis, and Y axis is oriented to respect the right-hand rule. This reference system rotates around the X axis when the telescope's elevation angle changes.

Unless otherwise indicated, all the components of the elevation structure are referred to the Elevation Coordinate System, while all the other components will refer to the Global Reference System.

3.3 Element Types

The Telescope Global FE model has been built by using the following ANSYS element types:

Element type	Formulation	Items	Average mesh size
Beam188	Quadratic	Structural beams members	30 mm
Mass21	-	Non-structural point masses (e.g., motors, bearings, mirrors etc.)	-
Shell181	Linear	Plated or thin-walled structures; thin-walled beams	30 mm 15 mm for pipes
Combin14	-	Actuators, azimuth and elevation bearings, motors, etc.	-
Solid186	Linear	Thick components	30 mm 50 mm for counterweights

Table 1 – Element types

Mesh quality has been checked for quality errors with the SHPP,ON and CHECK command by Ansys, and no errors are found. The mesh quality metrics are reported in the following table:

Table 2: Mesh quality table

Mesh Quality	Value
Min	0.06
Max	1.0
Average	0.88
STD deviation	0.14

The average mesh quality is quite high, 0.88 on a scale from 0 to 1 (higher is better).

3.4 Material Models

Only one material model is used to model the entire structure of the telescope, that is European structural steel S355J2.

A 5-15% density increase was applied to different components, so to consider the non-modelled mass of the welding, wiring, painting, etc. and make the total mass on-pair with the non-simplified model.

The properties of S355J2 steel are listed below:

355J2 Steel:

- Young Modulus: EX=210e9 N/m^2
- Poisson Ratio: NUXY=0.3
- CTE: ALPX=12e-6 $°C^{-1}$
- Density (nominal): DENS=7850 kg/m^3

- Yield Strength: σ_y = 355 MPa
- Ultimate Strength: σ_u = 490 MPa

The various density increases, adopted with respect to steel nominal, so that the mass of the different parts of the telescope structure FEM model is equal or greater to the CAD mass, are shown in the following figure:

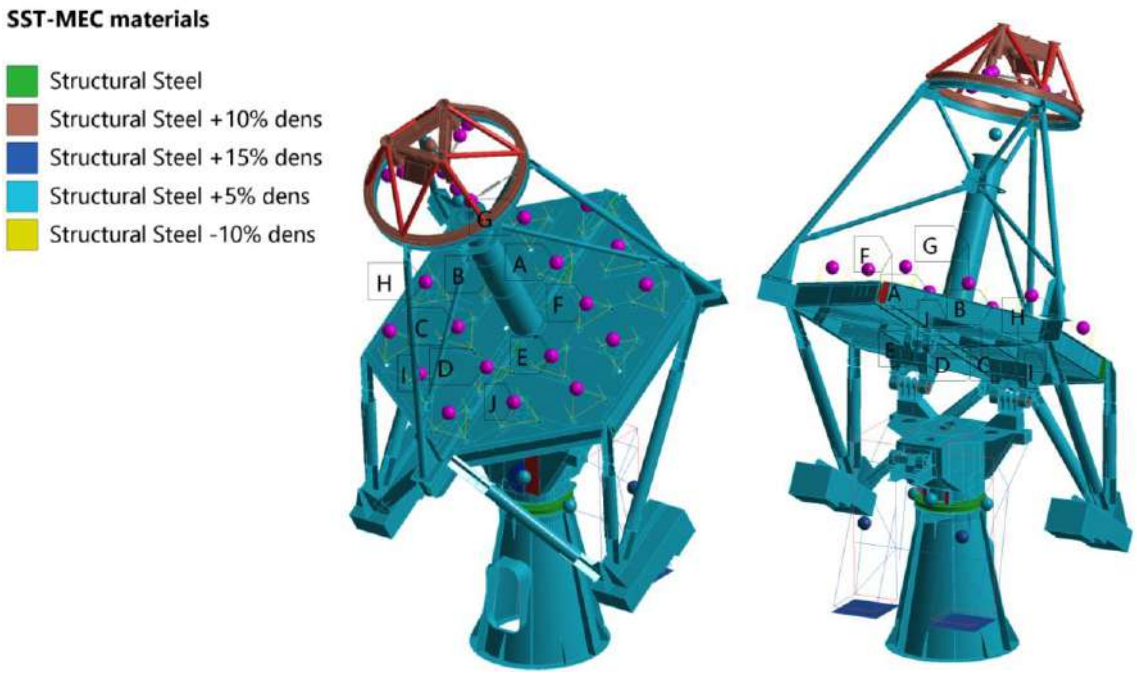

Figure 3-2: FEM model materials

Most of the telescope is modelled with structural steel featuring a density increase of 5% w.r.t. nominal.

3.5 Mass and Inertia of the FE Model

The mass and moments of inertia of the FE model are shown in the table below:

Item	Mass [kg]	Moments of inertia		
		Ixx [kg m^2]	Iyy [kg m^2]	Izz [kg m^2]
Mount - Base	1 673	-	-	-
Mount - Azimuth assembly	3 512	-	-	-
Optical Support Structure	12 043	42 200		
Rot Telescope - EL. 90°deg	15 555	-	-	43 234
Rot Telescope - EL. 60°deg		-	-	48 189
Rot Telescope - EL. 20°deg		-	-	48 312

Rot Telescope - EL. 0°deg		-	-	48 490
Total Telescope	17 228	-	-	-

Table 3 – mass and moments of inertia of the FE model

Moments of inertia are about the Global Reference System.

Detailed list of component masses in the subassemblies:

Item	Mass from FE model [kg]	Mass from 3D model [kg]
M2	170	170
M2 load spreader	99	112
M2 shields	40	33
M2 bus	326	328
M1 segments	180	180
M1 segments support assembly (including M1 actuators)	536	514
M1 dish	3696	3465
Mast + Central tube	835	706
Counterweights	5903	5059
Camera	100	100
M1 shields	130	116
PMC	10	10
EL bearings (EL struct)	32	32
EL bearing supports (EL struct)	191	240
Optical Support Structure	**12043**	**11065**

Table 4 – Mass budget Optical Support Structure

Item	Mass from FE model [kg]	Mass from 3D model [kg]
AZ fork	1353	1100
AZ Gearmotors	320	222

Item	Mass from FE model [kg]	Mass from 3D model [kg]
Cabinets	500	350
EL bearing supports (AZ struct)	118	110
EL motor	100	96
Ladder	12	11.5
Stow PIN AZ	100	74.5
Stow PIN EL	100	38
Cabinet support structures	355	350
Az bearing (rotating)	76	66
Azimuth Assembly	**3 512**	**2418**

Table 5 – Mass budget Mount - Azimuth structure

Item	Mass from FE model [kg]	Mass from 3D model [kg]
Az bearing (fixed)	98	96
Base structure	1555	1597
Door	20	17
Total rotating structure	**15 555**	**13483**
Total Telescope	**17 220**	**15193**

Table 6 – Mass budget telescope

3.6 FE Model

This section presents in detail the FE model of the telescope and its components, with descriptions of the assumptions made for each individual subsystem and the types of elements that have been used case-by-case.

The Telescope Mechanical Structure subdivision is given in [AD1], however, for the sake of the FE modelling, it is convenient to divide the telescope into three main assemblies:

- Mount, whose main elements are the base structure, the azimuth structure and the mount drive mechanisms, which is conveniently subdivided into:
    - Mount - Base: that is the fixed part of the structure, which has the task of supporting the entire telescope and connecting it to the ground.
    - Mount - Azimuth assembly: that is the assembly of rotating structures about the azimuth axis and that have the function of connecting the elevation assembly to the base.
- Optical Support Structure (OSS): this assembly has the task of supporting the optical components and the acquisition camera. In addition, in this assembly there are

counterweights that adequately balance the entire structure, while ensuring the residual torque needed to keep the elevation actuator in traction under every condition. It is composed by the M1 Dish, the OSS Upper Structure, the counterweights, and the M2 Support Structure.

The entire FE model, with the names of the main substructures of the telescope, is shown in the following images:

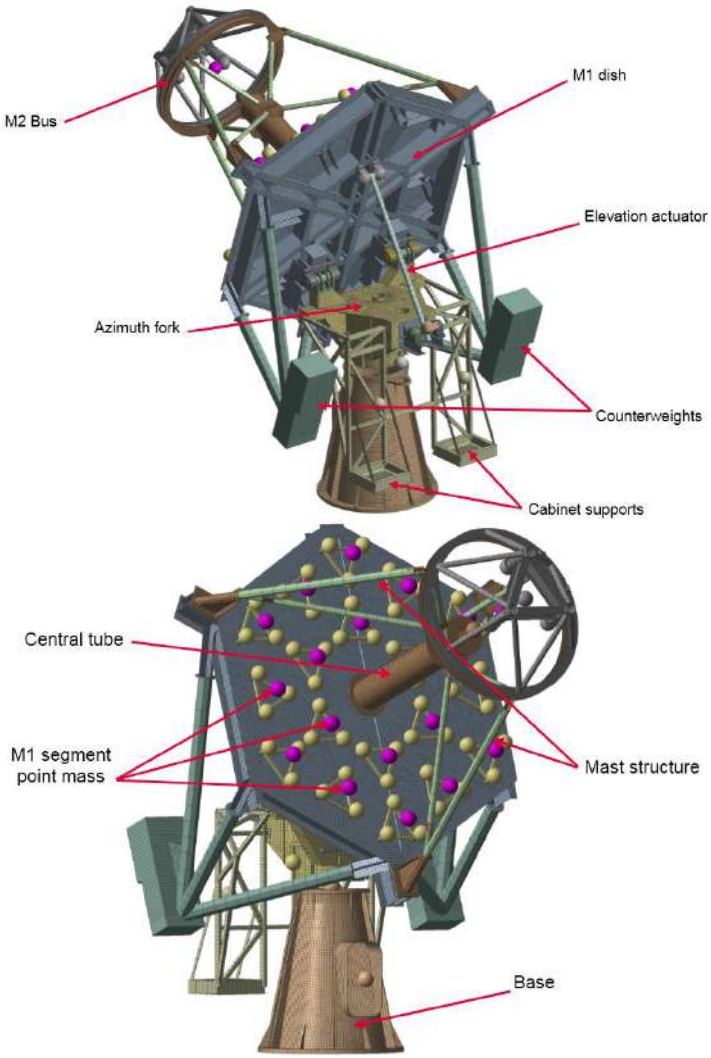

Figure 3-3 – Front and Rear global view of the FE model

In order to adequately describe and understand the overall behavior of the telescope, four different angles of elevation were considered in the analyses (named: EL 90°, EL 60°, EL 20°, EL 0°). These angles were chosen because:

- EL 90°: Telescope pointing to zenith. This angle represents one of the two telescope mobility extremes.
- EL 60°: It has been chosen this angle in the analysis, both to have a further intermediate position to evaluate the behavior of the telescope, and because it represents the statistically most used elevation angle during the observations.
- EL 20°: The 20° elevation angle represents the lower limit of the observing range.

- EL 0°: Telescope pointing to horizon. This is the parking position of the telescope. It will be in this position when it is not in an observation session.

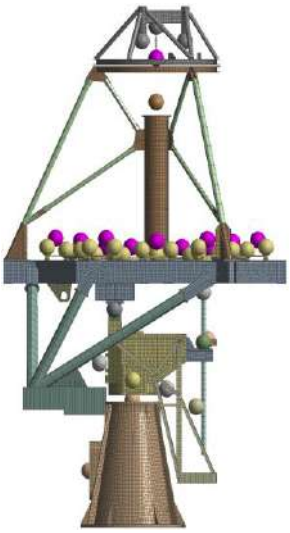

Figure 3-4 – Model with elevation angle of EL 90°

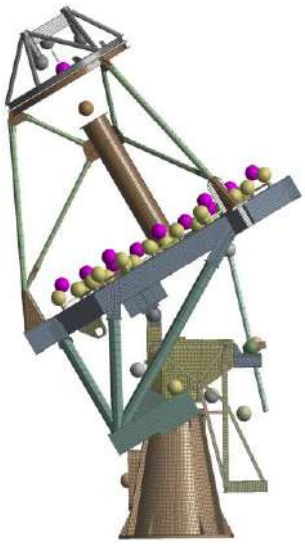

Figure 3-5 – Model with elevation angle of EL 60°

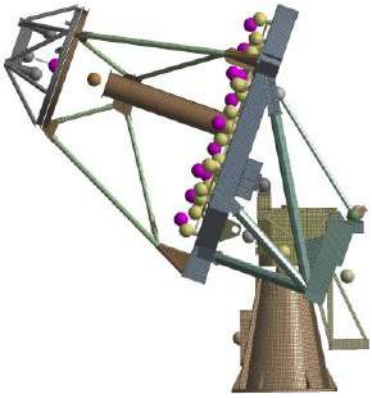

Figure 3-6 – Model with elevation angle of EL 20°

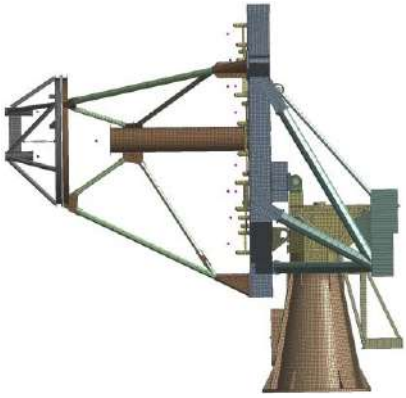

Figure 3- 3-7– Model with elevation angle of EL 0°

With reference to the images and the nomenclatures shown in the previous figures, the various subassemblies of the telescope are described below, with the assumptions and schematizations made case-by-case.

3.6.1 Mount – Base

The "Base" structure has the function to adequately support the entire telescope, and to act as a link between the mobile part and the ground. It houses at the top the azimuth bearing, whose stiffness characteristics are described in section 3.6.3 of RD1, the crown gear on which the pinions of the azimuth motors will hold, and the slot dedicated to housing the pin of the stow Pin. It is possible to access it inside, through a door, in order to carry out inspection and maintenance operations.

The structure is modeled with Shell elements for all the components consisting of sheet metal or having a dimension much smaller than the other two. Beam elements were used to model the two horizontal beams supporting the internal floor. Two concentrated masses have been added to take into account the masses of the access door (20kg) and of the azimuth bearing (98 kg), both placed in the center of gravity of the respective components.

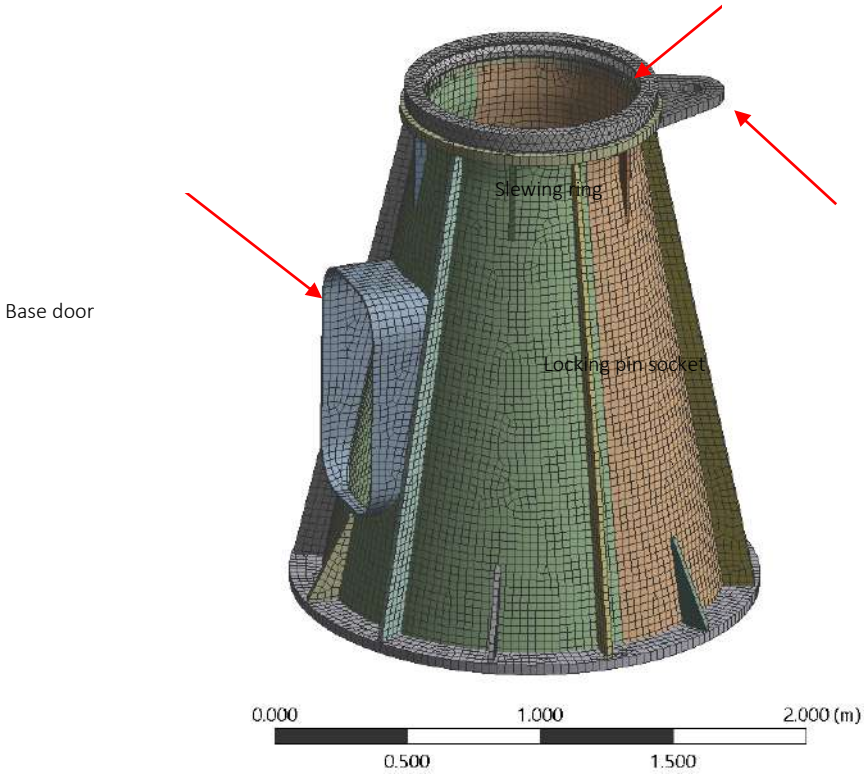

Figure 3-8 – Base

The constraint with the ground was modeled by imposing a null displacement to all the nodes falling in the outer ring of the base surface, as shown in the image below:

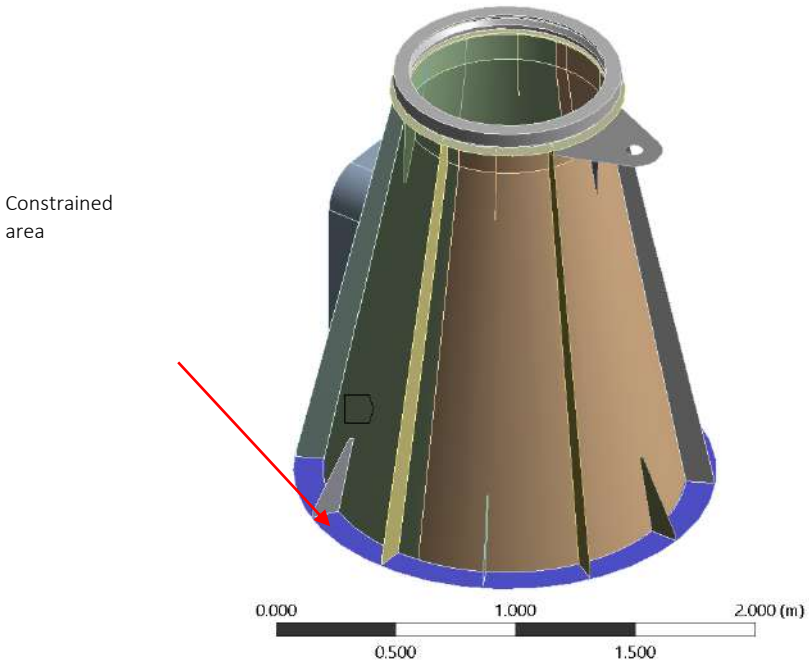

Figure 3-9 – Area of the Base bonded to the ground

3.6.2 Mount – Azimuth Assembly

The azimuth assembly was designed to support the entire elevation structure and connect it to the base. This component is composed by the azimuth fork, that is the main structural element of the assembly on which are anchored:

- the reticular structure used to support the cabinets (dedicated to the housing of electrical components)
- the support structure of the elevation actuator
- the two azimuth gear motors
- the elevation and azimuth stow pins
- the assembly housing the bearings and the encoder of the elevation axis.

The junction between the parts was generated by joining the mid-surfaces extracted from the 3D CAD model, in order to obtain imprints between surfaces and edges, so that the mesh is continuous. The mechanical components that find accommodation on the azimuth fork, but which do not contribute structurally, have been schematized with concentrated masses.

Where it has not been possible to join together the mid-surfaces of the plates due to the thicknesses of the same or for geometrical causes or due to the different nature of the FEM elements to be joined, contact elements have been used.

To allow the free rotation of some components, around a specific axis, "revolute" contacts have been used.

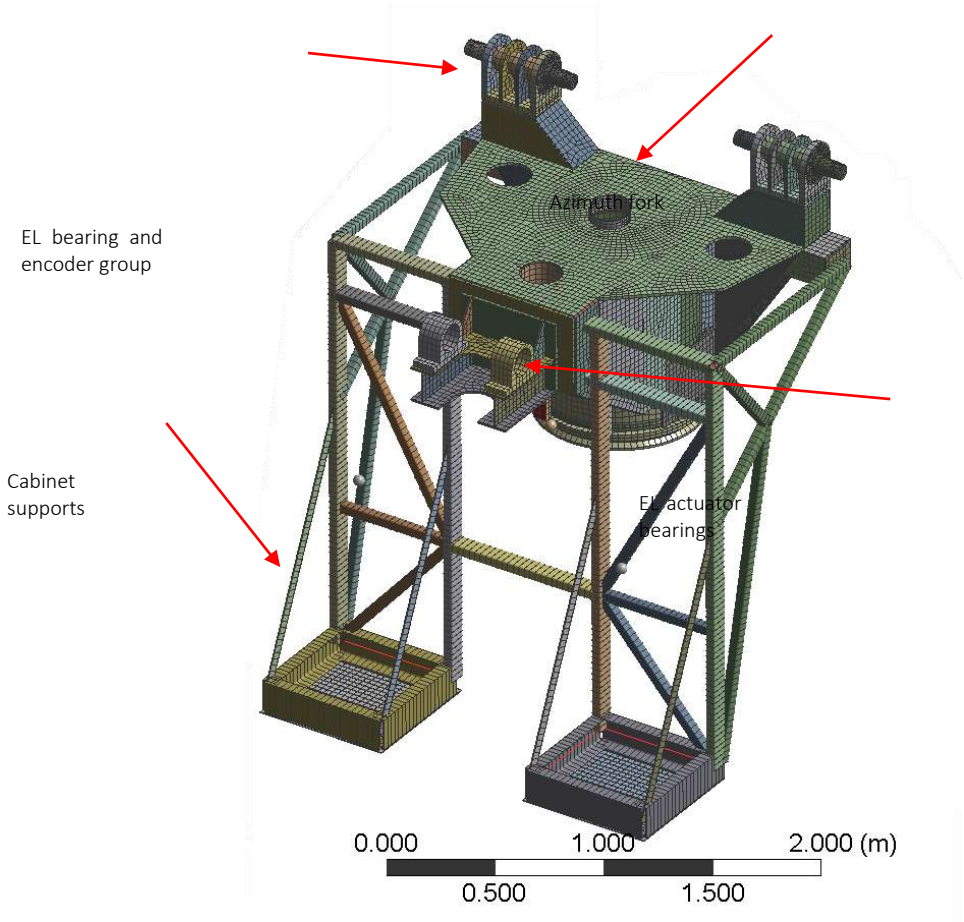

Figure 3-10 – Azimuth assembly

The various assemblies shown in the image above are described in detail below:

3.6.2.1 Azimuth fork & EL bearing encoder group

The azimuth fork has been modeled with shell elements for all components consisting in plates, sheets, or having a dimension much smaller than the other two, while 3D solid elements were used to schematize the parts with significant thickness placed at the interface points of the stow pins.

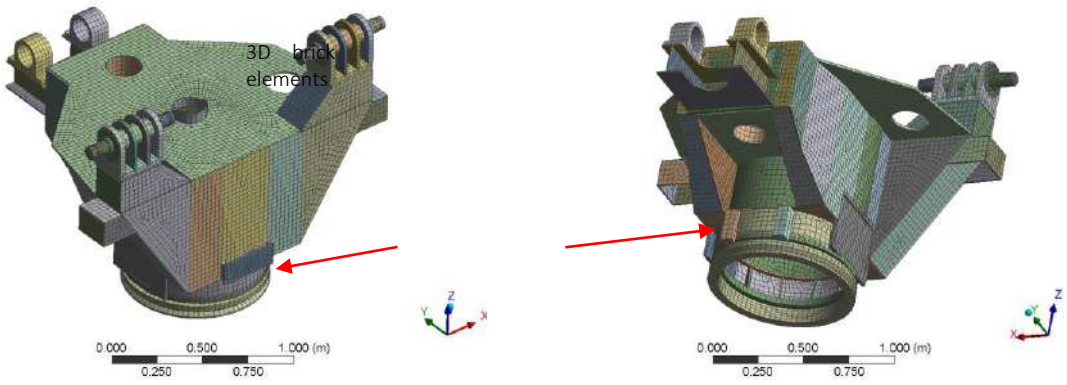

Figure 3-11 – Components modelled with Solid 3D elements

The junction between the parts was generated by joining the mid-surfaces extracted from the 3D CAD model, in order to obtain imprints between surfaces and edges, so that the mesh is continuous. The components mounted on the azimuth fork, except for those which are not structural elements, have been modelled with concentrate masses. In particular, were modelled with point masses the two azimuth motors, and the elevation and azimuth stow pins.

The torsional stiffness of the azimuth motors was modeled with a torsion spring acting between the two interface surfaces of base and azimuth fork, with an elastic constant equal to 2.721e + 008 N · m/°, calculated taking into account the stiffness provided by the manufacturer and the reduction ratio between the crown gear and the pinion.

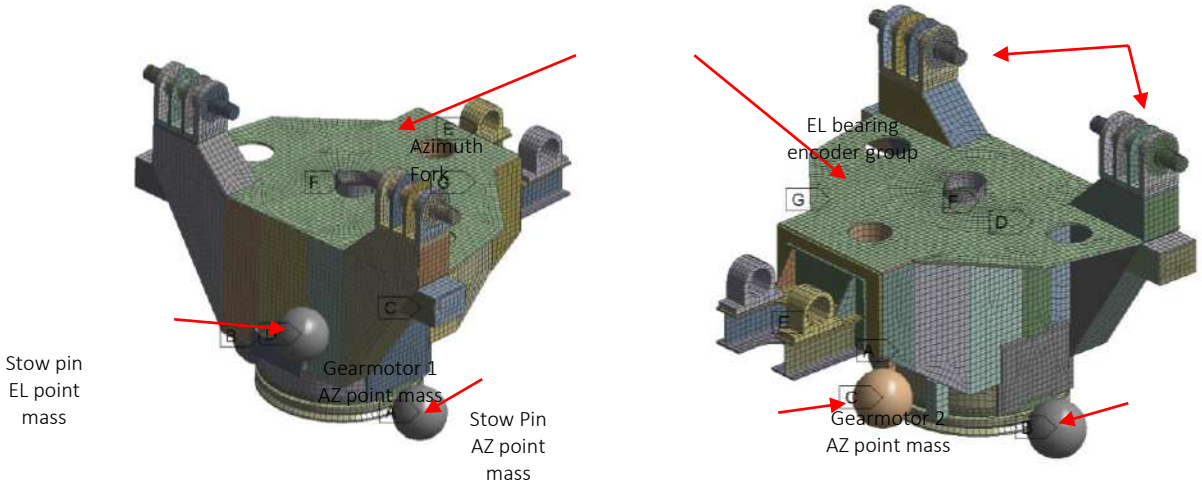

Figure 3-12 – Azimuth fork and EL bearing encoders group

3.6.2.2 Cabinet support

The reticular support structure of the cabinets has been modeled by Beam elements, whose sections and location in the model are shown in the table below.

The two flat surfaces at the base of the cabinets were modeled with shell elements, while the connecting flanges with the azimuth fork were modeled with solid 3D elements.

The masses of the two cabinets have been modelled as concentrated masses, placed in the center of gravity of the element and connected each one to the respective 4 beams UPN160 by means of contact elements.

Where the continuity of the mesh between the components could not be obtained, either for geometric reasons or for the diversity of the FEM elements to be connected, "bonded" contact elements were used.

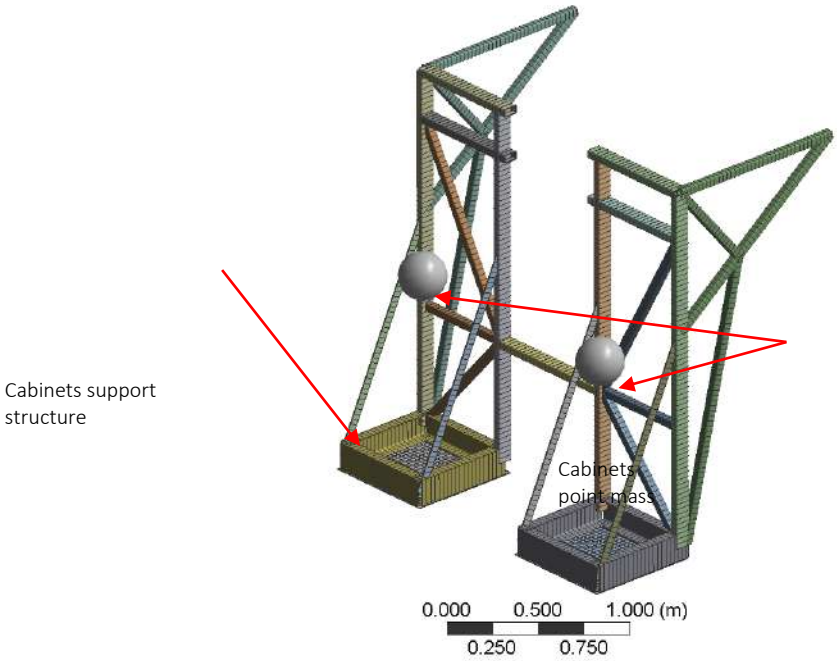

Figure 3-13 – Reticular support structure for cabinets

Sections and location of beams:

Cross-section plot	Cross-section description	Relevant beam members
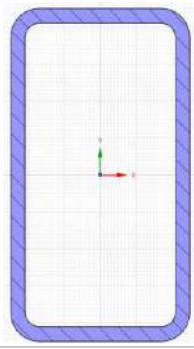	Rectangular sect. 90x50x4 mm	
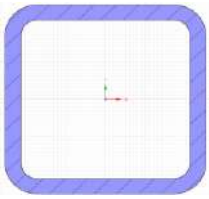	Square sect. 50x50x4 mm	

Cross-section plot	Cross-section description	Relevant beam members
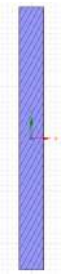	Rectangular sect. 50x5 mm	
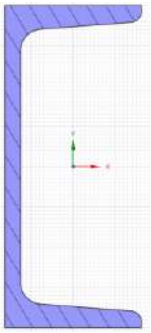	UPN160	

Table 7 – Sect. beams in the cabinets reticular support structure

3.6.2.3 Elevation actuator assembly

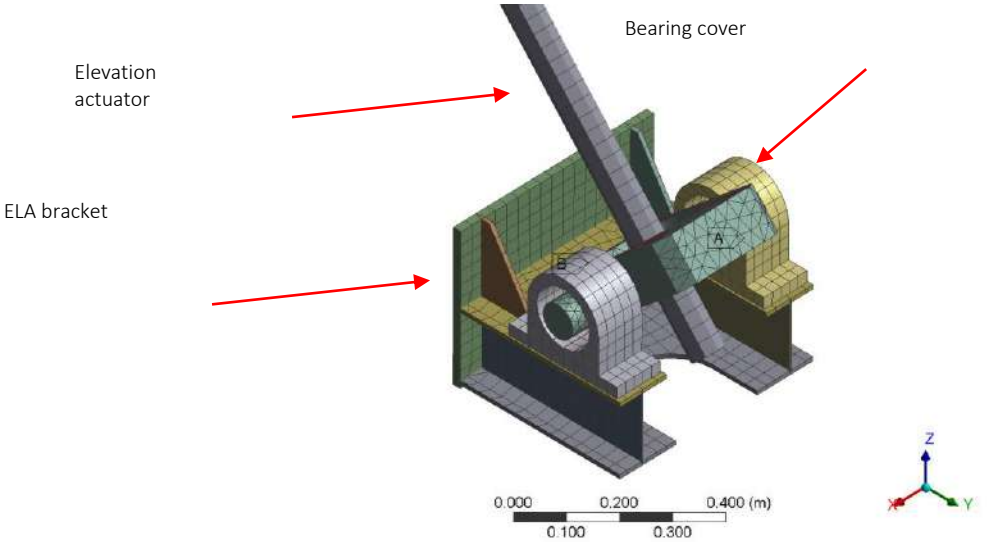

Figure 3-14 – Elevation actuator assembly

This assembly is composed of a steel structure made up of plates, which have been modeled by Shell elements. It has the purpose of supporting the elevation actuator and unloading a part of the weight of the elevation assembly on the azimuth fork, which falls on the actuator itself.

The mass of the motor and the masses of the two bearings were modeled with distributed masses, while the elevation actuator was schematized with a Beam element.

The axial stiffness of the actuator has been introduced by a Spring element, whose rigidity depends on the stroke of the actuator itself (L), therefore variable with the angle of elevation.

The value of the spring stiffness was obtained using the following empirical formula:

$$K = \frac{1000}{\left(\left(\frac{1}{1030478}\right) + \left(\frac{L}{875467086}\right)\right)}$$

Which allowed to obtain the following results, for the four different elevation angles used in the analyses:

Elevation angle	L [mm]	Stiffness [N/m]
90°	626	5.933E+8
60°	1466	3.781E+8
20°	2319	2.763E+8
0°	2636	2.512E+8

Table 8 – EL actuator stiffnesses

Sections and location of beams:

Cross-section plot	Cross-section description	Relevant beam members
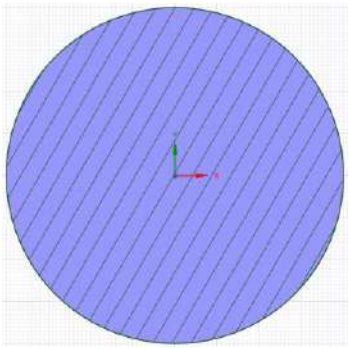	Circular sect. 80 mm	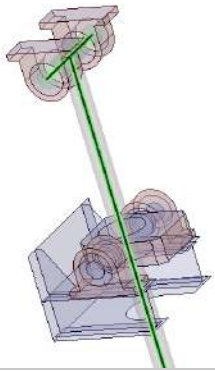

Table 9 – Elevation actuator beams sect.

3.6.3 Optical Support Structure

The OSS is designed to adequately accommodate and support the optics and the Cherenkov Camera, so as to guarantee the required alignment and pointing specifications.

The assembly consists of a reticular structure, which connects the support of the primary mirror, M1 dish, to the support of the secondary mirror, M2 Bus. On them are placed the optics, the camera, the counterweights and the elevation bearings. The junction between the various parts was generated by joining mid-surfaces extracted from the 3D CAD model, in order to obtain a continuous mesh. Where it was not possible to join the mid-surfaces due to the thicknesses of the plates or for geometrical issues or due to the different nature of the FEM elements to be joined, it has been used contact elements.

The components placed on the elevation assembly that do not contribute structurally, such as the optics, the cameras, and the supports of the mirrors, have been schematized with concentrated masses.

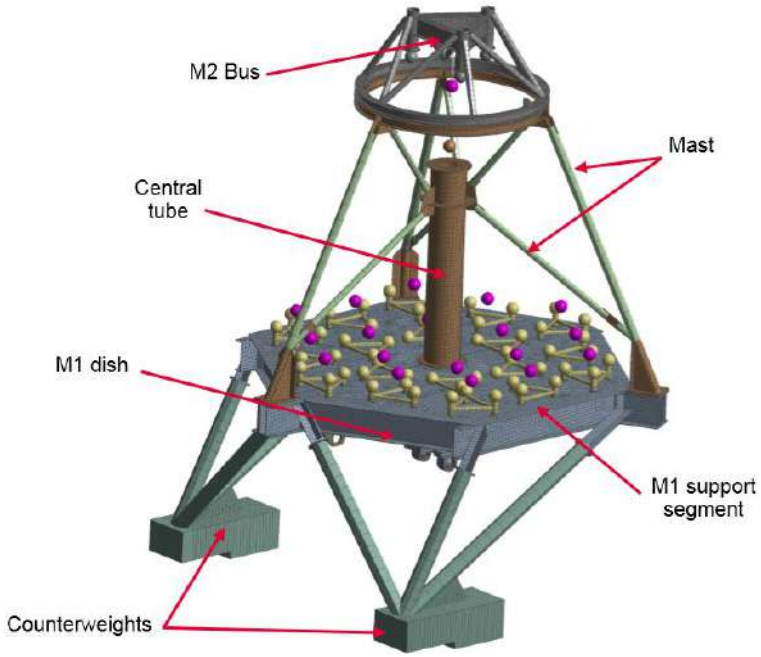

Figure 3-1 Elevation assembly

The various assemblies shown in the image above are described in detail below.

3.6.3.1 M1 Dish

"M1 Dish" is composed of a structure of UPE and IPE beams arranged to form a hexagonal shape and stiffened by other beams arranged in a radial direction. Three of the six radial beams extend beyond the limit of the hexagonal shape, to accommodate on their top the anchors of the reticular structure, connecting with the M2 Bus.

The M1 Dish design included in the present FEM model corresponds to the OP option, which is herein analyzed to establish an updated SST baseline, based on the validation given by the results of the present report.

The upper part of the structure formed by the beams, is covered by a 6 mm thick plate on whose surface are placed the triangular structures of supporting the segments of the primary mirror.

On the lower part, there are a series of stiffening ribs, the box supporting the bearings, and the interface flanges with the counterweights beams.

Figure 3-2 M1 dish

The mid-surfaces of the components, extracted from the 3D CAD design, were modeled with two-dimensional Shell elements. The structural continuity and the joint between the parts were guaranteed by imposing an imprint between the contact surfaces so as to obtain a continuous mesh.

On the other hand, where the mid-surfaces of the plates could not be joined together due to geometrical issues or due to the different nature of the FEM elements to be joined, contact elements have been used.

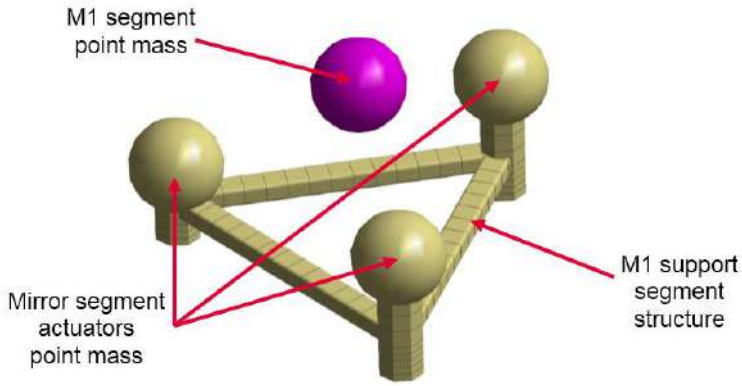

Figure 3-3 Primary mirror segment support structure

The 18 triangular support structures of the M1 mirrors were modeled by Beam elements, while both the mass of the segment and the masses of the actuators were modeled with concentrated masses.

The concentrated mass of the mirror segment has been linked to the supporting triangles by spring elements acting in the 3 directions. The springs have elastic constants such as to describe the axial and lateral behavior of the mirror actuators.

In particular:

K_{axial} = 1.388E+9 N/m

$K_{lateral}$= 6.310E+7 N/m

Sections and location of beams:

Cross-section plot	Cross-section description	Relevant beam members
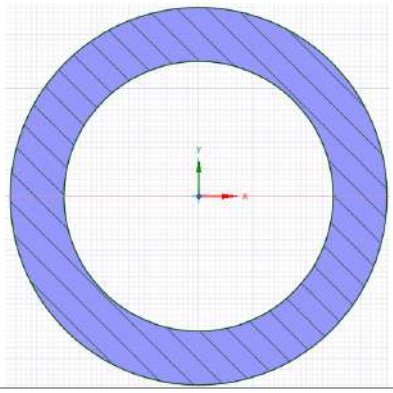	Circular sect. 70x10 mm	
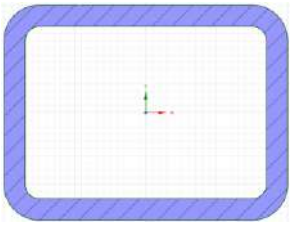	Rectangular sect. 40x30x3 mm	

Tab. 3-1: Sect. beams present on the support structures of the M1 segments

3.6.3.2 M2 Support Structure

The M2 Bus is the support and containment structure of the secondary mirror. It is formed by a circular ring with a double "T" section in the lower part, and a triangular structure made of double "T" profiles in the upper part. To connect the two portions there are a series of circular section tubular beams.

The triangular structure acts as a support for both the secondary mirror supports and the telescope pointing camera (PMC).

The structure has been modeled entirely by two-dimensional Shell elements, with the exception of the circular section tubular beams that have been modeled by Beam elements.

The masses of the secondary mirror, the load-spreaders and the PMC camera, have been modeled with concentrated masses positioned in the respective centers of gravity.

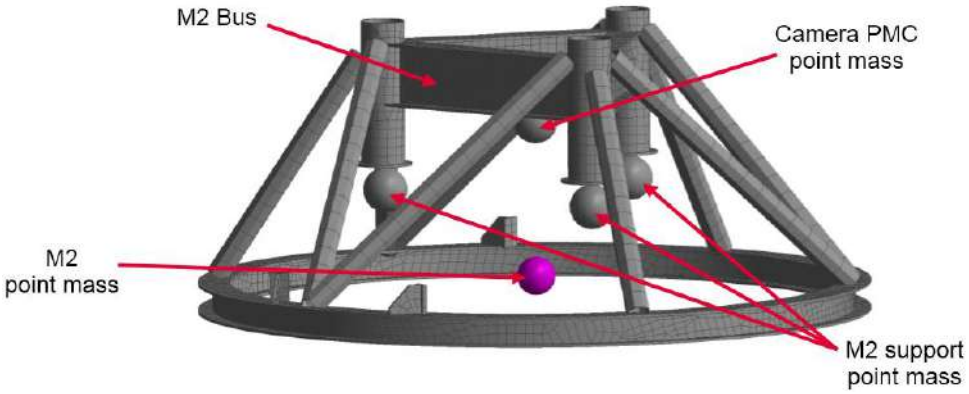

Figure 3-4 M2 bus assembly

The concentrated mass, representative of the secondary mirror M2, has been linked to the M2 Bus structure by spring elements acting in the 3 directions, having elastic constants such as to describe the axial and lateral behavior of the mirror load spreader. In particular:

K_{axial} = 3.768E+9 N/m

$K_{lateral}$= 1.145E+8 N/m

Stiffness values have been established by local FEM models of the actuators.

Sections and location of beams:

Cross-section plot	Cross-section description	Relevant beam members
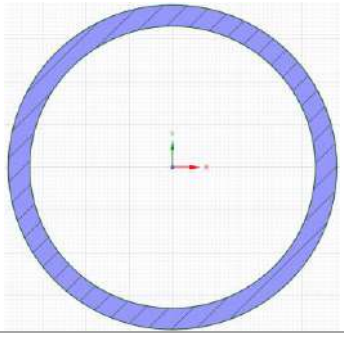	Circular sect. 76.1x10 mm	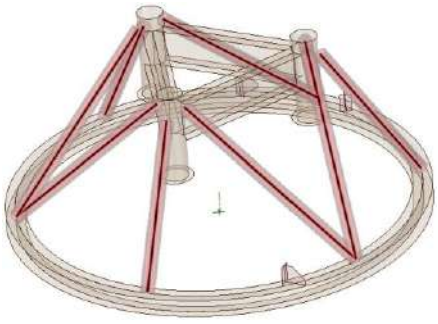

Tab. 3-2: Sect. beams on the M2 Bus

3.6.3.3 Mast and central tube

This structure is designed to adequately connect the two units that support the optics, M1 Dish and M2 Bus, and is made up of circular hollow section beams arranged radially at about 120° from each other. Two of the three structures are not perfectly radial but point out from the geometric center of the assembly, to give torsional rigidity.

There is a central tubular structure, called "Central tube", on top of which the Cherenkov camera is housed.

On the top there is the "Top ring", a circular ring with a double "T" section on which the M2 Bus is fixed.

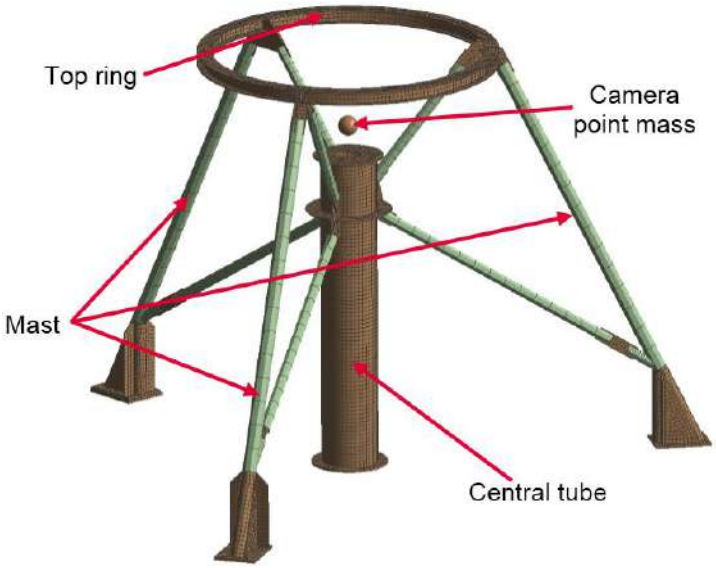

Figure 3-5 Elevation beams + Mast

In the FE model, the Top ring, the Mast and the parts that connect the tubular beams to the M1 dish have been modeled by shell elements, while all the beams have been modeled by Beam elements.

Sections and location of beams:

Cross-section plot	Cross-section description	Relevant beam members
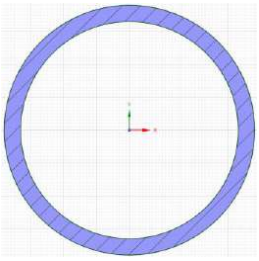	Circular sect. 76.1 x10 mm	

Cross-section plot	Cross-section description	Relevant beam members
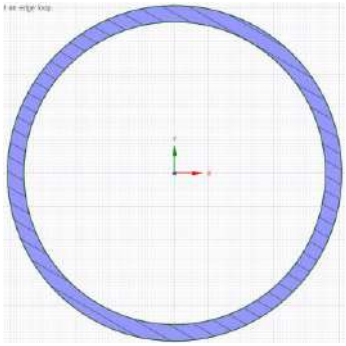	Circular sect. 101.6x10 mm	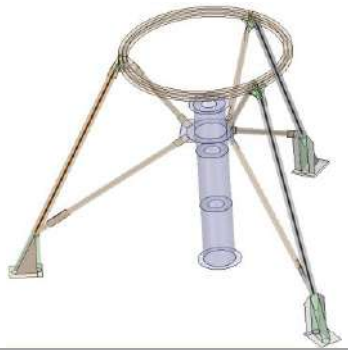

Tab. 3-3: Elevation beams beams sect.

3.6.3.4 Counterweights

The counterweights are necessary to adequately balance the elevation structure about the respective axis of rotation. In order to prevent the chance of buckling of the elevation actuator screw, a residual torque, between 3000 and 4500 Nm, is ensuring that the elevation actuator always be in traction.

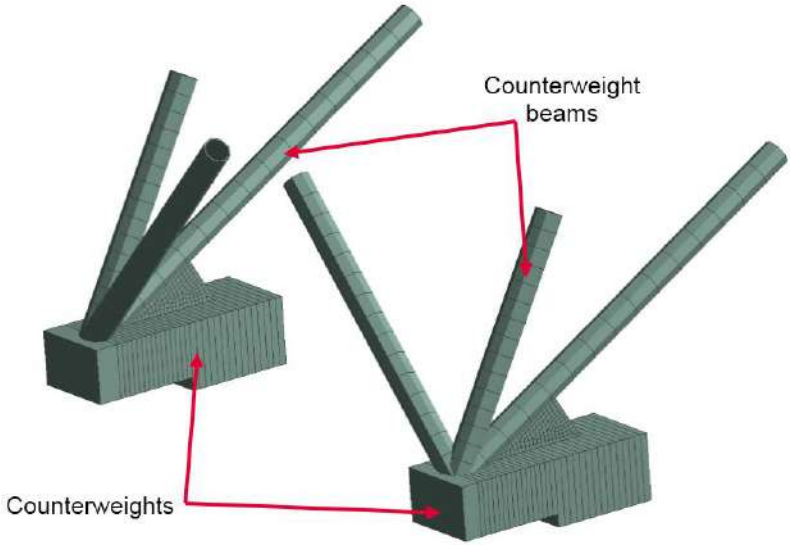

Figure 3-6 Counterweight assembly

The counterweights are formed by a series of steel plates, which in the model have been modelled with beams, whose section groups together the whole of all these plates. Each one of them is connected to the M1 dish structure, by 3 circular section tubular beams, schematized in the FE model with Beam elements.

Since the counterweights are very simple elements, which do not contain welding, cables, flanges, etc., the density of the material used to describe the mass, has NOT been increased by 10%.

Sections and location of beams:

Cross-section plot	Cross-section description	Relevant beam members
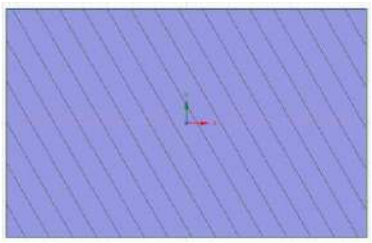	Rectangular sect. 350x550 mm	
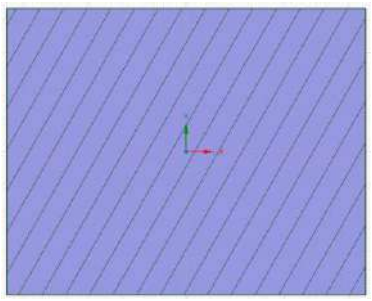	Rectangular sect. 435x550 mm	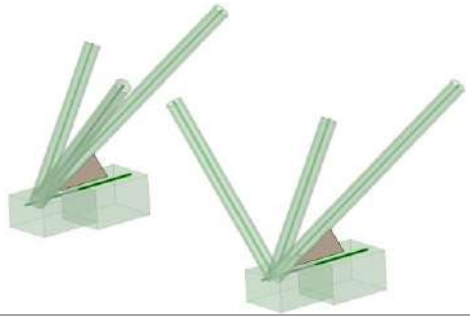
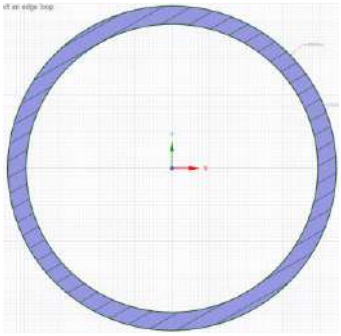	Circular sect. 177.8x10 mm	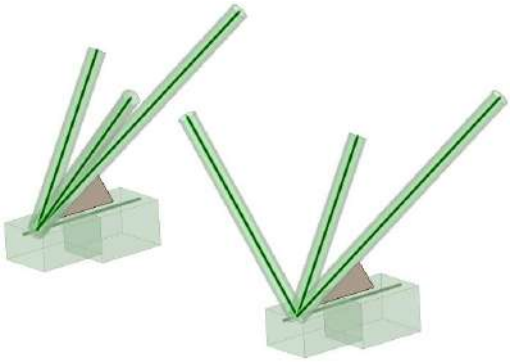

Tab. 3-4: Counterweight beams sect.

3.6.4 Summary of masses and stiffness adopted

These mechanical components have been schematized by spring elements having adequate rigidity, such as to guarantee their elastic representativeness: elevation actuator, azimuth motors, and M1 and M2 supports.

The table below summarizes all the stiffness values used in the FE model:

Component	Schematization	Stiffness		
		Axial [N/m]	Lateral [N/m]	Torsional [Nm/°]
M1 supports	Axial spring	1.388E+9	6.310E+7	-

Component	Schematization	Stiffness		
		Axial [N/m]	Lateral [N/m]	Torsional [Nm/°]
M2 supports	Axial spring	3.768E+9	1.145E+8	-
Elevation actuator	Axial spring (EL 90°)	5.933E+8	-	-
	Axial spring (EL 60°)	3.781E+8	-	-
	Axial spring (EL 20°)	2.763E+8	-	-
	Axial spring (EL 0°)	2.512E+8	-	-
Azimuth motors	Torsional spring	-	-	2.721e+8

Table 10 – Stiffness values summary

All the stiffness values present in the FE model have been either obtained from the catalogs by the suppliers or hand calculated.

The azimuth bearing is a fundamental element for telescope behavior. Its stiffness affects both the main frequencies of the telescope and the tracking error. For this reason, it is important that the FE model correctly simulates the bearing, its rigidity and the connection with the structure.

The azimuthal bearing has been modeled by axial springs acting in the three Cartesian directions, and by two torsion springs acting along orthogonal axes respect to the vertical. The values of these stiffnesses depend to the applied loads, and have been evaluated by the bearing supplier, with a dedicated non-linear FE model, considering both the operating and survival loads.

In the following tables are reported the values estimated by the supplier:

Stiffness Matrix	x [m^{-1}]	y [m^{-1}]	z [m^{-1}]	yz [rad^{-1}]	zx [rad^{-1}]
Fx [N]	7.01 ^{E}09	-2.21 ^{E}07	-4.96 ^{E}06	-9.10 ^{E}06	1.91 ^{E}09
Fy [N]	-2.21 ^{E}07	8.56 ^{E}09	3.57 ^{E}09	-1.24 ^{E}09	9.10 ^{E}06
Fz [N]	-4.96 ^{E}06	3.57 ^{E}09	1.56 ^{E}10	1.20 ^{E}09	2.04 ^{E}07
Myz [Nm]	-9.10 ^{E}06	-1.24 ^{E}09	1.20 ^{E}09	1.45 ^{E}09	3.75 ^{E}06
Mzx [Nm]	1.91 ^{E}09	9.10 ^{E}06	2.04 ^{E}07	3.75 ^{E}06	1.19 ^{E}09

Table 11 – Azimuth bearing stiffness matrix

In order to take into account the mass of all the components that are housed on the telescope, but which do not contribute structurally, a series of concentrated or distributed masses, placed in the center of gravity of each one of the systems to be represented, were inserted into the FE model, and are summarized in the following table:

Component	Mass [kg]		Type	Sub-assembly location
M2 supports	3x33	9	Concentrated mass	M2 Bus
Cabinet	2x250	500	Concentrated mass	Cabinet reticular

Component	Mass [kg]		Type	Sub-assembly location
Camera	1x100	100	Concentrated mass	Mast
EL bearings	8x4	32	Concentrated mass	M1 Dish
Stow Pin AZ	1x100	100	Concentrated mass	AZ fork
Stow Pin EL	1x100	100	Concentrated mass	AZ fork
M2	1x170	170	Concentrated mass	M2 Bus
EL motor	1x100	100	Concentrated mass	EL actuator assembly
AZ gear-motor	2x160	320	Concentrated mass	AZ fork
PMC	1x10	10	Concentrated mass	M2 Bus
Base Door	1x20	20	Concentrated mass	Base
M1 shield	8x15+1x10	130	Distributed mass	M1 Dish
Ladder	1x12	12	Concentrated mass	Cabinet reticular
M2 shield	1x40	40	Distributed mass	M2 Bus
M1 mirror segment	18x10	180	Concentrated mass	M1 Dish

Table 12 – Summary of concentrated and distributed masses

Only the main components have been modeled with concentrated or distributed masses in this model. All the other masses due to minor components such as cables, pipes, paint, etc., are already included in the 10% margin on steel density.

3.7 Model Integrity Checks

3.7.1 Free-rotor modes

This check aims to verify that removing the constraints on the telescope moving parts, the model finds a number of near-to-zero frequency modes equal to the degree of freedom of the machine (two in this case, Elevation rotation and Azimuth rotation).

The analysis was performed on the 60° elevation case, freeing the azimuth rotation and the actuator screw linear movement.

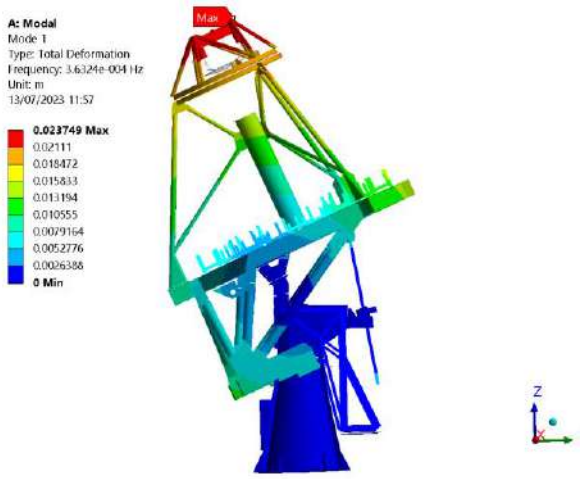

Figure 3-15 – Mode 1, Elevation rotation

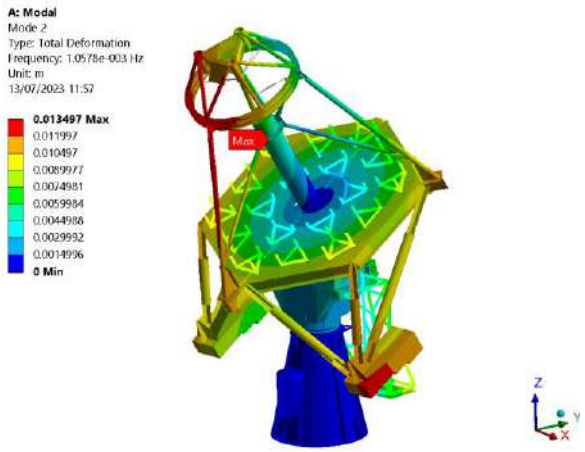

Figure 3-16 – Mode 2, Azimuth rotation

3.7.2 Free body modes

This analysis aims to verify that the model without any constraint (nothing to fix it to the ground and no internal constraint between moving parts) has a number of near-to-zero frequencies modes that equals 6 + # of d.o.f. of the machine, in this case 8 d.o.f.

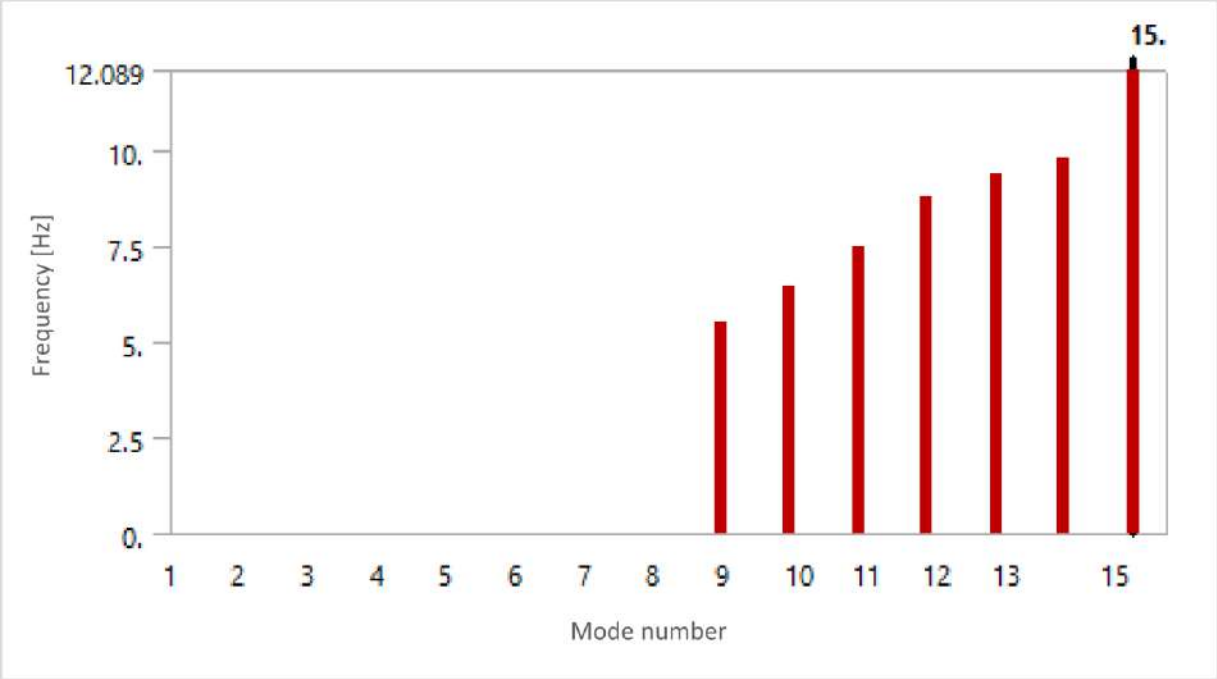

Figure 3-17 – Modes distribution for the free-body analysis

The model has no overconstraints both external and internal. The first non-zero frequency is for Mode 9, and it corresponds to the oscillation of the counterweights support arms.

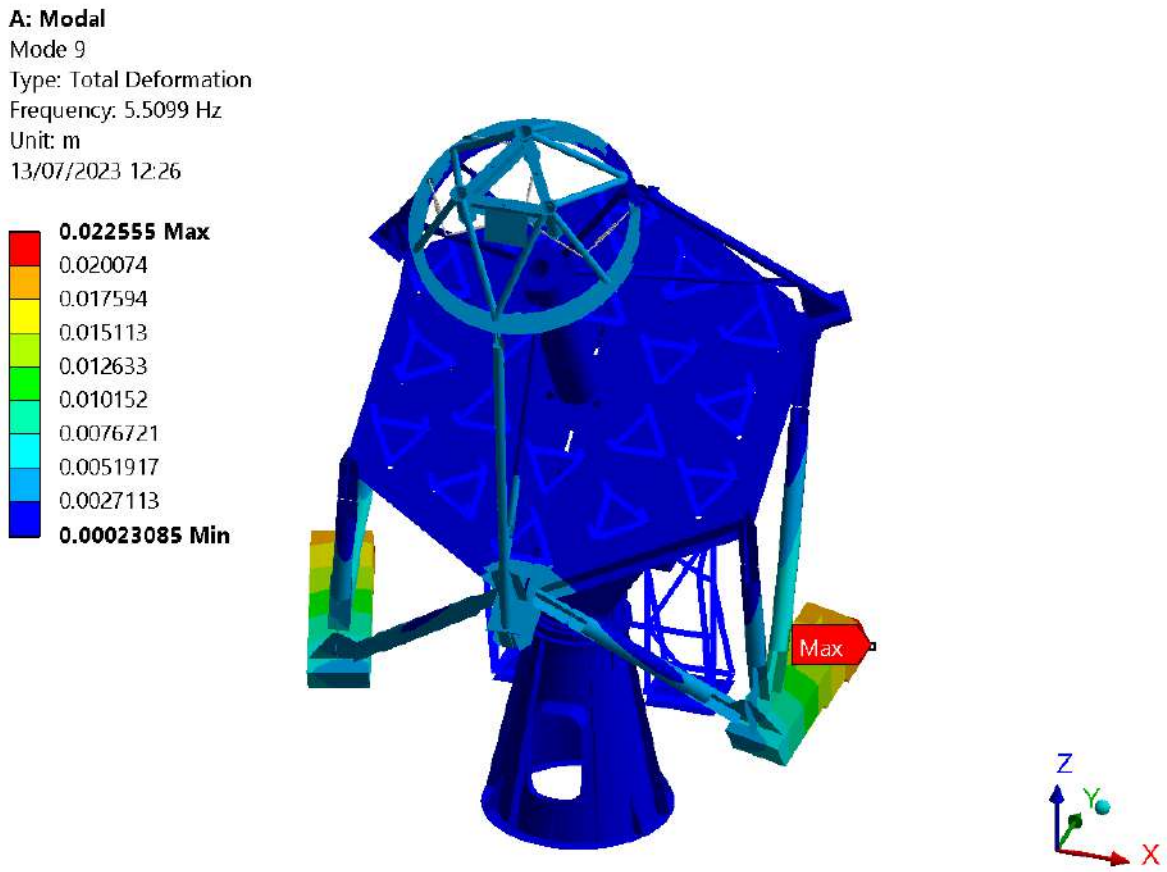

Figure 3-18 – First non-zero frequency mode for the free body modal analysis

3.7.3 1g Acceleration on each direction

These analyses aim to check if the fixed support that grounds the telescope has a well modeled behavior. Three different analysis each with the gravity acceleration in a different main direction are computed, and the expected result is that for each one the constraint has a force reaction that equals the weight of the whole telescope.

Here are reported the results of the three analyses performed:

Acceleration direction	Fx	Fy	Fz
-Z	-5.7915e-005 N	1.2468e-004 N	**1.6887e+005 N**
-Y	-1.2425e-004 N	**1.6887e+005 N**	2.254e-003 N
-X	**1.6887e+005 N**	3.3067e-003 N	-1.2048e-003 N

Table 13 – Reaction forces with gravity in the main three directions

It is possible to see that the three reaction forces are always the same, and dividing by 1g, the weight of the telescope is obtained (17220 kg).

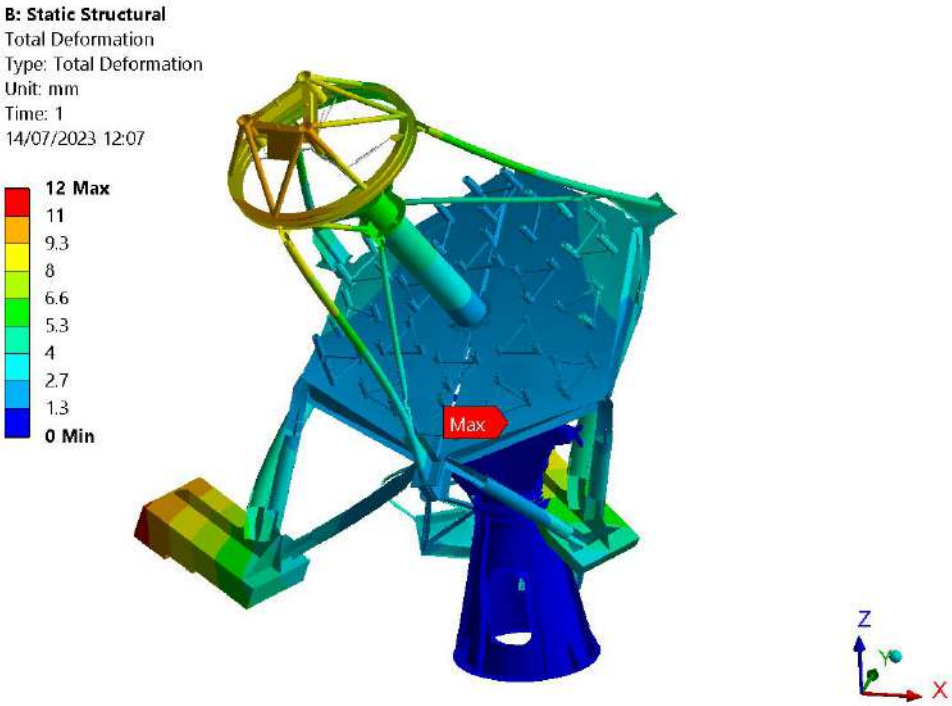

Figure 3-19 – -x direction gravity

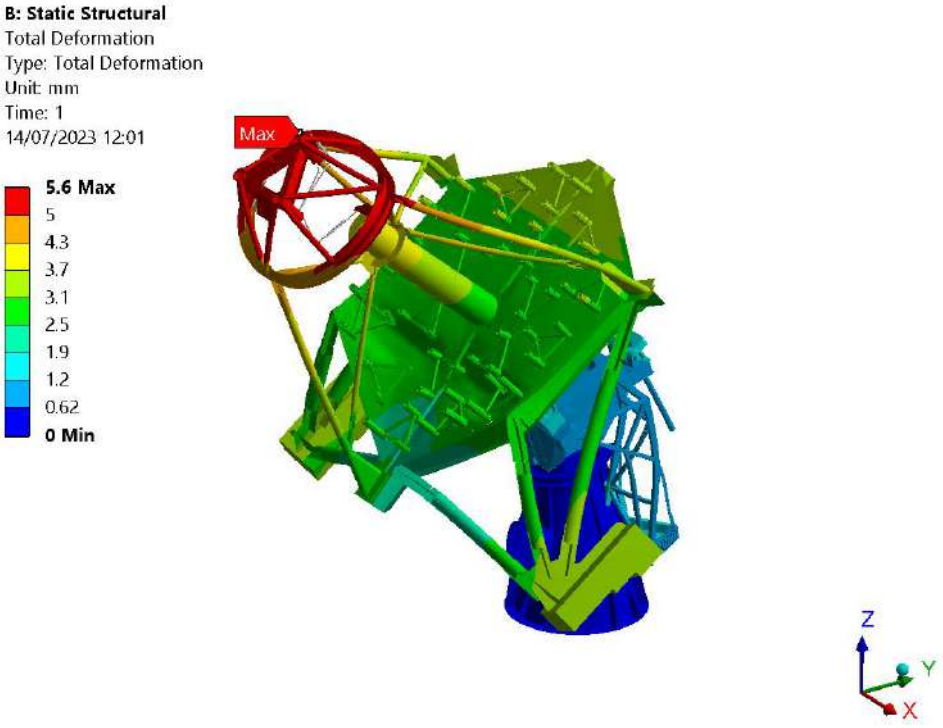

Figure 3-20 – -y direction gravity

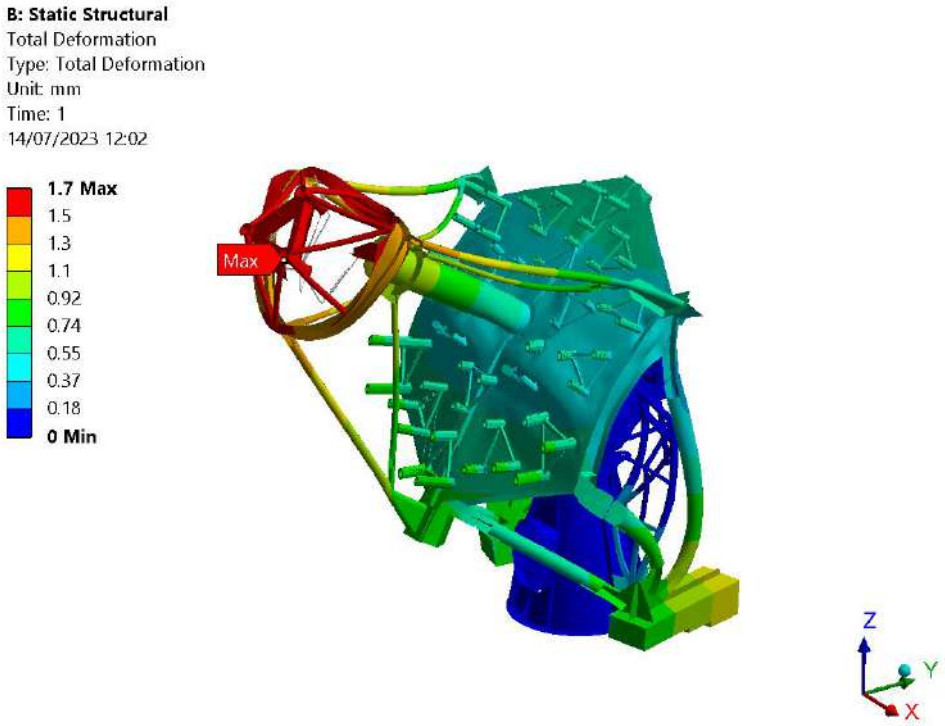

Figure 3-21 – -z direction gravity

4 Analyses and Results

This analysis report aims to show that the proposed telescope design meets the structural requirements according to the technical specifications.

All the performed analyses and the relative results are presented in this section.

The verification criteria, the analysis procedures and the load cases are shown below, while all the results are shown and discussed later.

4.1 Verification Method and Criteria

The structural verification of the telescope was performed according to the limit states method (LSD), as indicated in the [RD3].

The structure is required to satisfy the Ultimate Limit State (ULS) criterion.

According to [RD5]-1-1 §6.2, as far as structural resistance verifications are concerned, the elastic verification criterion is:

$$\sigma_{VM} < f_y/\gamma_{M0};$$

Where:

σ_{VM} : are the equivalent Von Mises stress

f_y : the yield stress of the material

γ_{M0} : safety factor = 1.

4.2 Analyses and Load Cases Description

The following analyses have been performed:

- Static analysis: Gravity load case
- Modal analysis: Locked rotor condition
- Response Spectrum Analysis: NCR Seismic Analysis

4.2.1 Gravity Load Case description

The effects of gravity were assessed by applying an acceleration of -9.8066 m/s^2 along the Z_G axis to the whole Telescope Structure.

4.2.2 Seismic Analysis description (NCR Earthquake)

The effects of seismic loads have been investigated by performing a modal response spectrum analysis, in order to verify the telescope structural resistance.

First the eigenfrequencies and the eigenmodes of the structure have been calculated by performing a modal analysis; then three Spectrum Analyses (one per each component of the seism action) have been performed, so to calculate the relevant modal response of each single mode.

The modal responses of the structure have been combined according to the Complete Quadratic Combination (CQC) method.

A critical damping ratio of 2% shall be assumed when calculating the seismic spectra, and behaviour factor q is set equal to 1.

Seismic spectra as s function of period shall be calculated according to the following formulae ([RD6] Part 1, section 3.2.2.2):

Period range	$S_e(T)$
$0 \le T \le T_B$	$a_g \cdot S \cdot [1 + T/T_B \cdot (\eta \cdot c - 1)]$
$T_B \le T \le T_C$	$a_g \cdot S \cdot \eta \cdot c$
$T_C \le T \le T_D$	$a_g \cdot S \cdot \eta \cdot c \cdot [T_C/T]$
$T_D \le T \le 4s$	$a_g \cdot S \cdot \eta \cdot c \cdot [T_C \cdot T_d/T^2]$

- $\eta = [10 / (5 + \xi)]^{1/2}$ (see also EC 8, Section 3.2.2.2)
- Se (T) is the elastic acceleration response spectrum in [g]
- T is the vibration period in [s]
- a_g Peak Ground Acceleration in [g]
- c is the ratio between the maximum and the peak ground acceleration
- T_B is the lower limit of the constant spectral acceleration branch in [s]
- T_C is the upper limit of the constant spectral acceleration branch in [s]
- T_D is the value defining the beginning of the constant displacement response range in [s]
- η is the damping correction factor
- ξ is the damping ratio in percent

The parameters for the calculation of the seismic spectra applicable to the No Collapse Requirement for the SST are the following, as per [AD2]:

- Peak horizontal ground acceleration at 5% damping ratio: 0.43g
- Peak vertical ground acceleration at 5% damping ratio: 0.26g
- 10% probability of exceeding these figures in 50 years (reference return period 475 years).

Other parameters for the seismic spectra calculation are reported in the following table:

- NCR SST (soft Soil. 5% damping)

Parameters	a_g	S	T_B	T_C	T_D	c
	[g]	[-]	[s]	[s]	[s]	[-]
Horizontal	0.43	1.70	0.10	0.35	2.00	2.5
Vertical	0.26	1.80	0.05	0.30	2.00	3.0

With these conditions, all systems shall meet the Collapse Prevention Limit state.

The seismic spectra at 2% damping ratio as a function of frequency is given in the following plot:

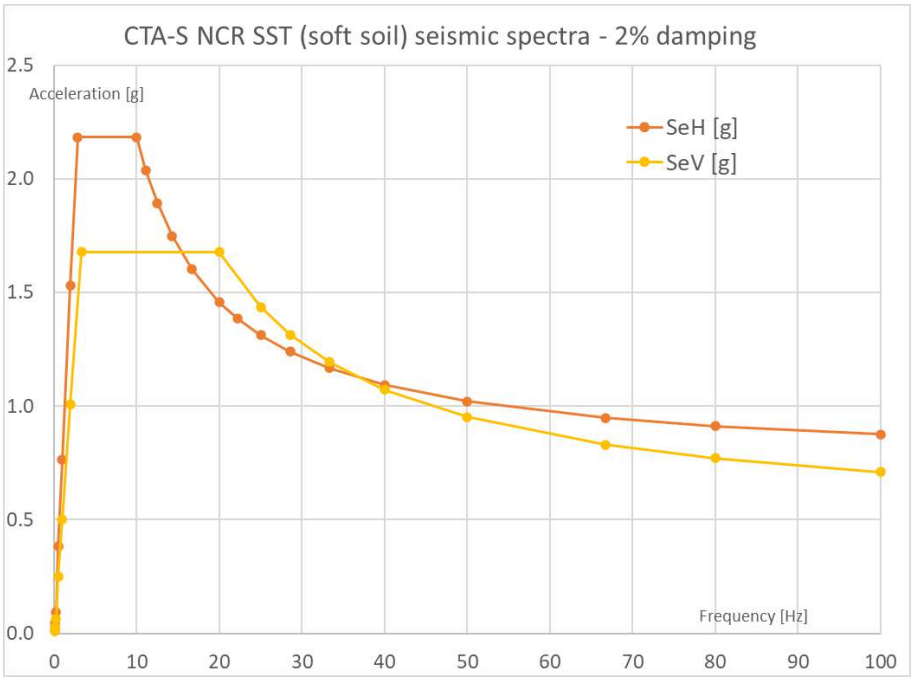

Figure 4-1: CTA South NCE seismic spectra for the SST

Summing up, the Earthquake analysis has been performed as follows:

- All modes of the telescope up to 50 Hz involved into the Modal Analysis
- Single Point Response Spectrum (SPRS) Analysis
- Modal response calculation with NCR acceleration response spectra for the reference site
- SRSS spatial combination of the three components of the seismic action

The mass of the modes of the telescope higher than 50 Hz has been taken into account by means of the "missing mass effect", that means by applying to the missing mass an acceleration equal to the PGA.

Two configurations of the telescope have been considered for the seismic analysis: the parking position, which is the most frequent telescope configuration, and the average observation angle of 60deg elevation.

4.3 Modal Analysis Results – Locked Rotor

This section describes the results of the modal analysis, in a locked rotor condition.

Below there is a summary of the results that compare the values of the first 15 frequencies of the telescope, in relation to the four angles of elevation considered in the analyses (90°, 60°, 20° and 0°). In addition, other information such as the modal mass involved in the single directions and the representative figures of the various vibration modes are present.

4.3.1 Elevation angle 90° (Zenith pointing)

Elevation angle 90°								
Mode	Freq [Hz]	Description	Modal mass %					
			X	Y	Z	rotX	rotY	rotZ
1	5.38	Counterweights opposite oscillation	21.7%	0.4%	0.2%	0.1%	11.4%	0.7%
2	5.46	Counterweights synchronous oscillation	7.0%	1.3%	0.7%	0.3%	3.6%	0.3%
3	6.20	EL assembly Z_G rotation	0.3%	0.0%	0.0%	0.0%	9.8%	82.6%
4	6.91	M2 bus torsion about ZEL	5.7%	0.0%	0.0%	0.0%	23.2%	2.8%
5	7.27	EL assembly tilting about X_G	0.0%	7.6%	1.7%	56.2%	0.0%	0.0%
6	8.15	EL assembly tilting about Y_G + torsion of M2 Bus	11.4%	0.0%	0.0%	0.0%	18.4%	4.3%
7	8.75	Cabinets truss structure	0.0%	0.3%	0.1%	0.1%	0.0%	0.0%
8	8.93	Cabinets truss structure	5.4%	0.0%	0.0%	0.0%	2.8%	0.1%
9	9.83	General structural deformations	0.0%	8.6%	0.6%	1.0%	0.0%	0.0%
10	10.27	General structural deformations	0.0%	47.4%	2.6%	8.2%	0.0%	0.0%
11	10.53	Actuator beam deformation	0.1%	0.2%	0.0%	0.0%	0.4%	6.4%
12	11.59	Actuator beam deformation	0.3%	0.0%	0.0%	0.0%	0.4%	0.0%
13	12.09	Local cabinet structure	0.0%	0.0%	0.0%	0.0%	0.0%	0.0%
14	12.09	Local cabinet structure	0.0%	0.0%	0.0%	0.0%	0.0%	0.0%
15	12.14	Local cabinet structure	0.0%	0.0%	0.0%	0.0%	0.0%	0.0%

Table 14 – Modal analysis results for EL 90°

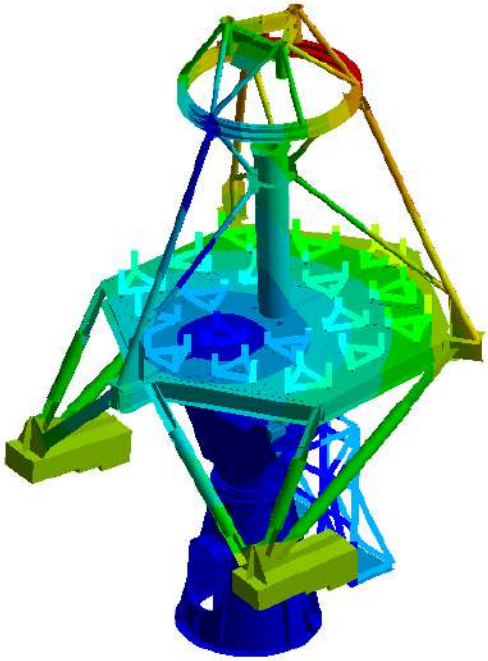

Figure 4-2 – EL assembly rotation about ZG – 6.20 Hz

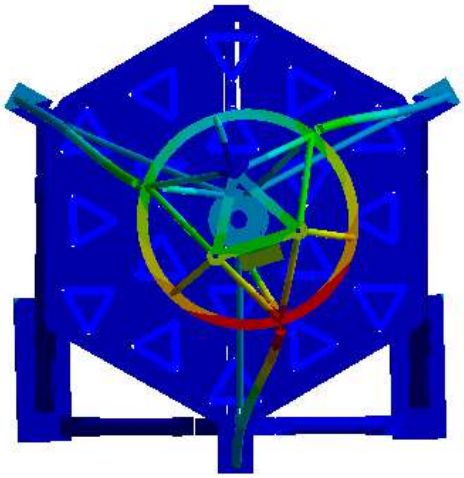

Figure 4-3 – M2 Bus torsion about ZEL – 6.91 Hz

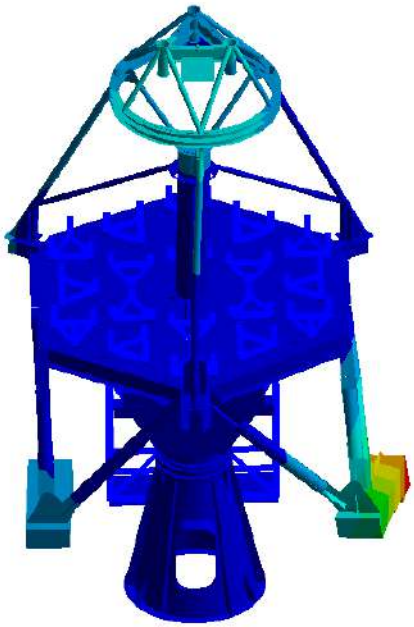

Figure 4-4 – Counterweights –5.38Hz

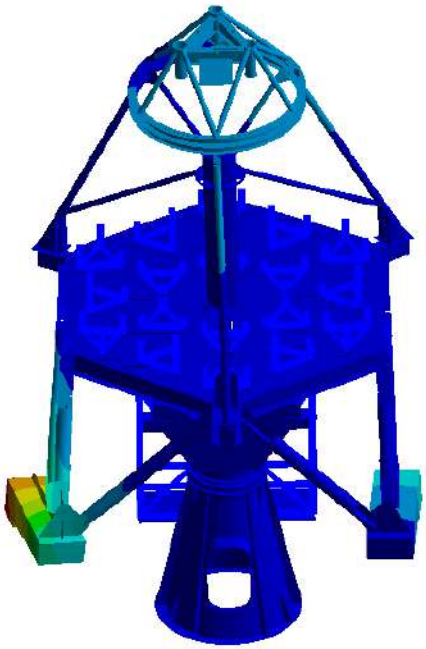

Figure 4-5 – Counterweights – 5.46Hz

4.3.2 Elevation angle 60°

Mode	Freq [Hz]	Description	Elevation angle 60° Modal mass % X	Y	Z	rotX	rotY	rotZ
1	5.27	Counterweights synchronous oscillation	23.4%	0.1%	0.0%	0.0%	8.0%	10.3%
2	5.43	Counterweights opposite oscillation	1.0%	3.3%	0.0%	0.0%	0.3%	0.5%
3	6.51	Torsion of EL assembly around ZEL	6.9%	0.0%	0.0%	0.0%	0.3%	65.9%
4	6.79	EL assembly tilt about X_G	0.0%	3.4%	1.0%	60.7%	0.0%	0.0%
5	6.90	EL assembly tilt about Y_G	4.6%	0.0%	0.0%	0.0%	52.3%	1.6%
6	7.90	Torsion of M2 Bus around ZEL	7.9%	0.0%	0.0%	0.0%	5.5%	14.4%
7	8.75	Cabinets truss structure	0.0%	0.2%	0.1%	0.2%	0.0%	0.0%
8	8.93	Cabinets truss structure	5.4%	0.0%	0.0%	0.0%	2.9%	0.0%
9	9.76	General structural deformations	0.0%	60.5%	0.0%	6.0%	0.0%	0.0%
10	10.23	General structural deformations	1.0%	0.1%	0.0%	0.0%	1.8%	2.8%
11	12.09	Local cabinet structure	0.0%	0.0%	0.0%	0.0%	0.0%	0.0%
12	12.09	Local cabinet structure	0.0%	0.0%	0.0%	0.0%	0.0%	0.0%
13	12.14	Local cabinet structure	0.0%	0.0%	0.0%	0.0%	0.0%	0.0%
14	12.17	Local cabinet structure	0.0%	0.0%	0.0%	0.0%	0.0%	0.0%
15	12.66	Cabinets truss structure	1.2%	0.0%	0.0%	0.0%	0.0%	0.4%

Table 15 – Modal analysis results for EL 60°

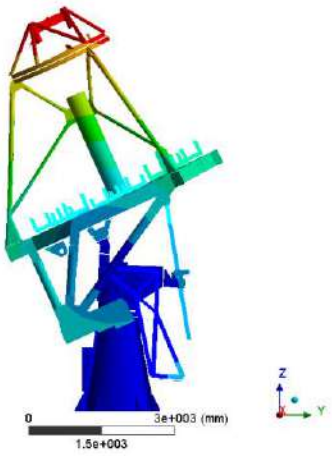

Figure 4-6 – EL assembly rotation about X_G – 6.79 Hz

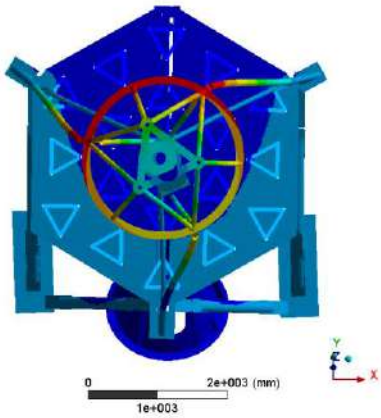

Figure 4-7 – M2 Bus torsion about Z_{EL} – 7.90 Hz

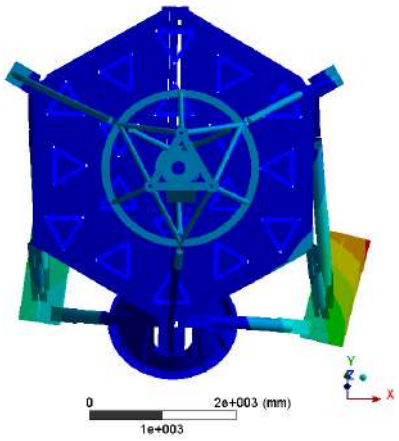

Figure 4-8 – Counterweight sync. – 5.27 Hz

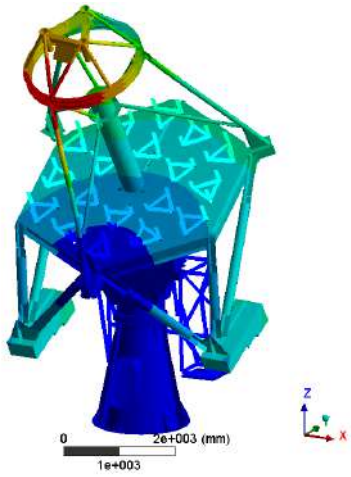

Figure 4-9 – EL assembly tilt about Y_G – 6.90 Hz

4.3.3 Elevation angle 30°

Elevation angle 60°								
Mode	Freq [Hz]	Description	Modal mass %					
			X	Y	Z	rotX	rotY	rotZ
1	5.08	Counterweight synchronous osc.	17.9%	0.0%	0.0%	0.0%	4.9%	32.7%
2	5.40	Counterweight opposite osc.	0.1%	3.5%	0.4%	0.6%	0.0%	0.4%
3	5.81	EL assembly tilt about X_G	0.0%	0.3%	0.4%	63.9%	0.0%	0.0%
4	6.35	Torsion of M2 Bus around ZEL	18.4%	0.0%	0.0%	0.0%	13.3%	44.9%
5	7.20	EL assembly tilt about Y_G + tors. of M2 Bus	0.6%	0.0%	0.0%	0.0%	36.4%	0.5%
6	8.03	Counterweights and M2 Bus torsion around ZEL	3.8%	0.0%	0.0%	0.0%	6.0%	16.7%
7	8.75	Cabinets truss structure	0.0%	0.1%	0.0%	0.3%	0.0%	0.0%
8	8.94	Cabinets truss structure	5.1%	0.0%	0.0%	0.0%	4.2%	0.0%
9	9.68	General structural deformations	0.0%	60.5%	1.9%	2.1%	0.0%	0.0%
10	10.30	General structural deformations	1.2%	0.0%	0.0%	0.0%	4.3%	1.0%
11	12.09	Local cabinet structure	0.0%	0.0%	0.0%	0.0%	0.0%	0.0%
12	12.09	Local cabinet structure	0.0%	0.0%	0.0%	0.0%	0.0%	0.0%
13	12.14	Local cabinet structure	0.0%	0.0%	0.0%	0.0%	0.0%	0.0%
14	12.17	Local cabinet structure	0.0%	0.0%	0.0%	0.0%	0.0%	0.0%
15	12.65	Cabinets truss structure	1.3%	0.0%	0.0%	0.0%	0.0%	0.4%

Table 16 – Modal analysis results for EL 60°

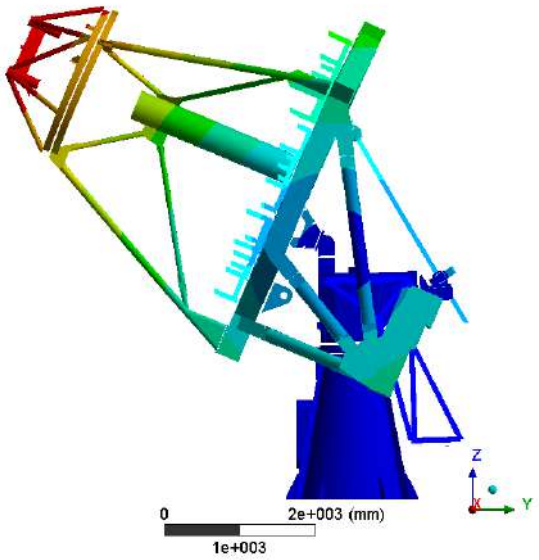

Figure 4-10 – EL assembly rotation about X_G – 5.81 Hz

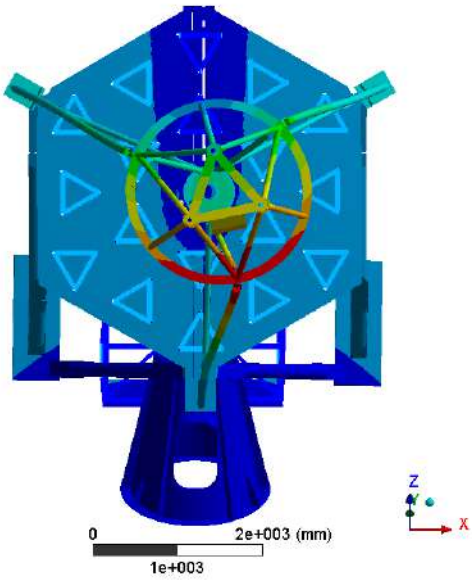

Figure 4-11 – M2 Bus torsion about Z_{EL} – 6.35 Hz

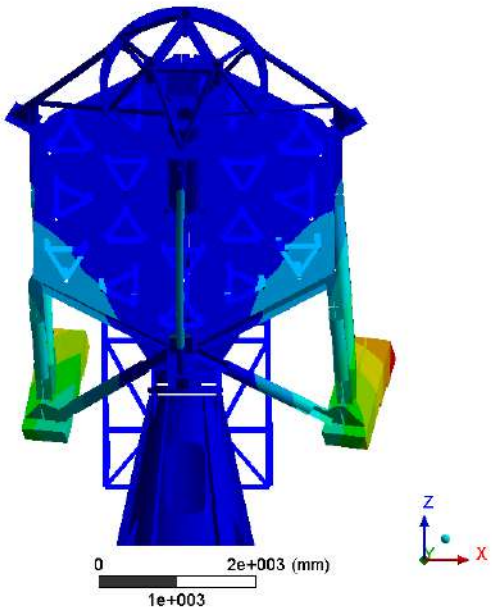

Figure 4-12 – Counterweight right – 3.67 Hz

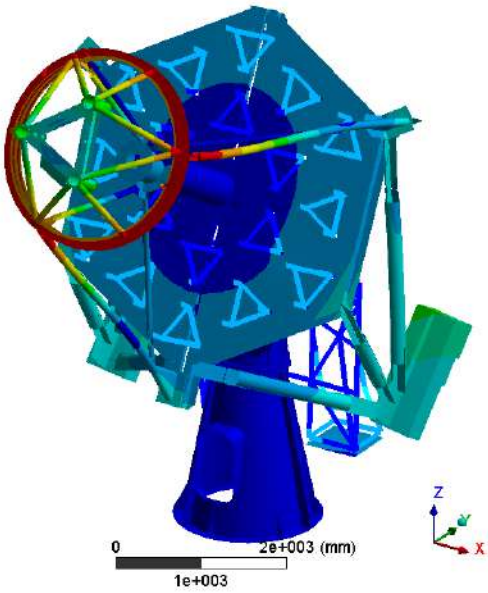

Figure 4-13 – EL assembly tilt about Y_G + tors. of M2 Bus and Counterweights – 6.49 Hz

4.3.4 Elevation angle 0° (Horizon pointing)

Elevation angle 0°								
Mode	Freq [Hz]	Description	Modal mass [%]					
			X	Y	Z	rotX	rotY	rotZ
1	4.30	EL assembly tilt about X_G	0.0%	0.0%	0.3%	65.7%	0.0%	0.0%

Elevation angle 0°								
Mode	Freq [Hz]	Description	Modal mass [%]					
			X	Y	Z	rotX	rotY	rotZ
2	4.90	Counterweights synchronous osc.	14.1%	0.0%	0.0%	0.0%	0.7%	46.0%
3	5.39	Counterweights opposite osc.	0.0%	1.7%	1.5%	0.2%	0.0%	0.3%
4	6.03	EL assembly rotation about Z_G	20.5%	0.0%	0.0%	0.0%	13.5%	44.0%
5	7.22	M2 Bus torsion about Z_{EL}	0.0%	0.0%	0.0%	0.0%	16.0%	0.1%
6	8.68	EL assembly torsion about Y_G	2.3%	0.0%	0.0%	0.0%	16.3%	6.5%
7	8.74	Cabinets truss structure	0.0%	0.1%	0.0%	0.4%	0.0%	0.0%
8	8.94	Cabinets truss structure	5.6%	0.0%	0.0%	0.0%	8.6%	0.1%
9	9.97	General structural deformations	0.0%	56.8%	5.9%	0.4%	0.0%	0.0%
10	10.38	General structural deformations	0.9%	0.1%	0.0%	0.0%	8.5%	0.1%
11	12.09	Cabinet local structure	0.0%	0.0%	0.0%	0.0%	0.0%	0.0%
12	12.09	Cabinet local structure	0.0%	0.0%	0.0%	0.0%	0.0%	0.0%
13	12.14	Cabinet local structure	0.0%	0.0%	0.0%	0.0%	0.0%	0.0%
14	12.17	Cabinet local structure	0.0%	0.0%	0.0%	0.0%	0.0%	0.0%
15	12.65	Cabinets truss structure	1.3%	0.0%	0.0%	0.0%	0.0%	0.3%

Table 17 – Modal analysis results for EL 0°

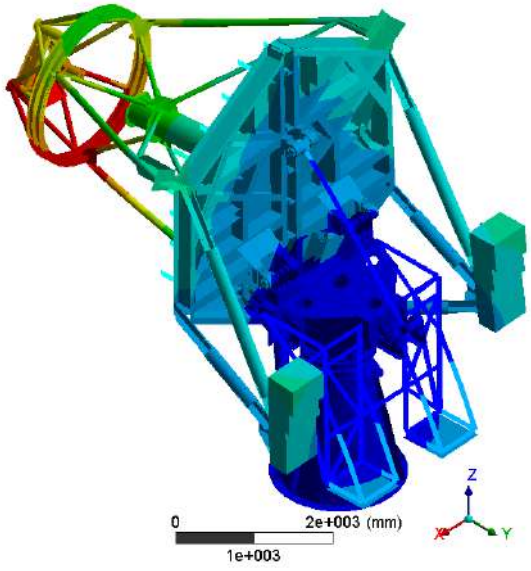

Figure 4-14 – EL assembly rotation about ZG – 6.03 Hz

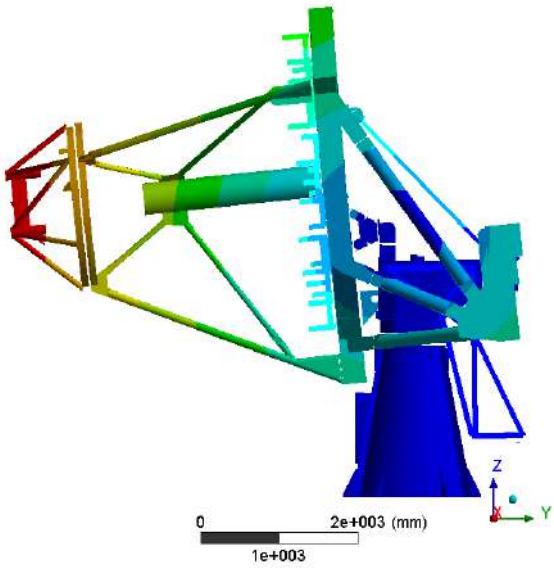

Figure 4-15 – EL assembly tilt about XG – 4.30 Hz

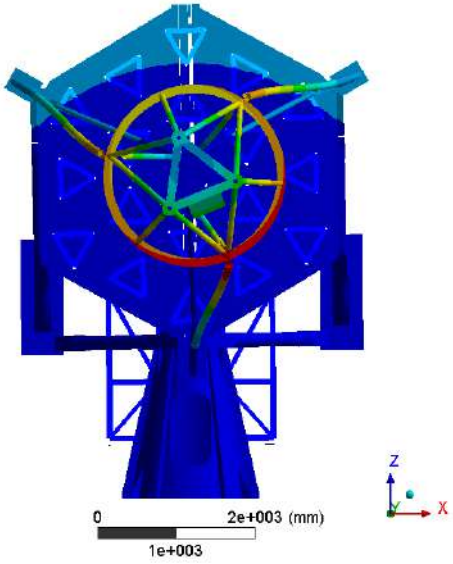

Figure 4-16 – M2 Bus torsion about ZEL – 7.22 Hz

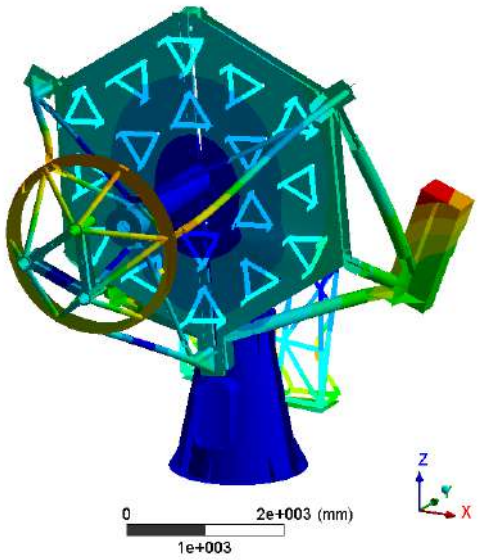

Figure 4-17 – EL assembly torsion about YG – 8.68 Hz

4.4 Static Analyses Results

The results of the static analyses are reported in this section, both as regards the stresses, and as regards the deformations of the structure with particular attention to the misalignments of the optics.

4.4.1 Static analysis: Stress

In the following, there is a summary of the results, which compares the maximum stress level assessed by the FE analysis with the allowable stress of the material, for all four angles of elevation taken into consideration.

In accordance with the verification criterion described in paragraph 4.1 and with the characteristics of the material used in the construction of the telescope (chapter 3.4), steel S355J0, whose yield stress is (for plate thickness up to 40 mm):

$$\sigma_y = 355\ N/mm^2$$

and the ultimate tensile strength is:

$$\sigma_u = 490\ N/mm^2$$

A summary table is given below containing the values of the peaks stress, calculated with the Von Mises criterion, and the related additional safety factors compared to yield (SF_y) and ultimate (SF_u) strengths.

Load case	Elevation angle [deg]	Telescope Structure				
		σVM,max [MPa]	SFy	notes	SFu	notes
Gravity	90	59.5	6.0	C	8.2	C
	60	51.7	6.9	C	9.5	C
	30	89.4*	4.0	C	5.5	C
	0	103*	3.4	C	4.8	C
SF=Additional Safety Factor C=Compliant *punctual stress						

Table 18 – Summary of static analyses: Stress

The results show that the maximum stress is well below the limit for all the considered cases, with SF_y = 4.8 as an additional safety factor. The minimum safety factor for static analysis shall be 1.5. The maximum stress due to gravity (110.2 MPa) located on the support box for the elevation bearings, is not able to induce permanent deformations in the structure of the telescope.

In the next paragraphs the results of the static analyses are reported in greater detail, subdivided by the four different angles of elevation:

4.4.1.1 Elevation angle 90°, Gravity (stress)

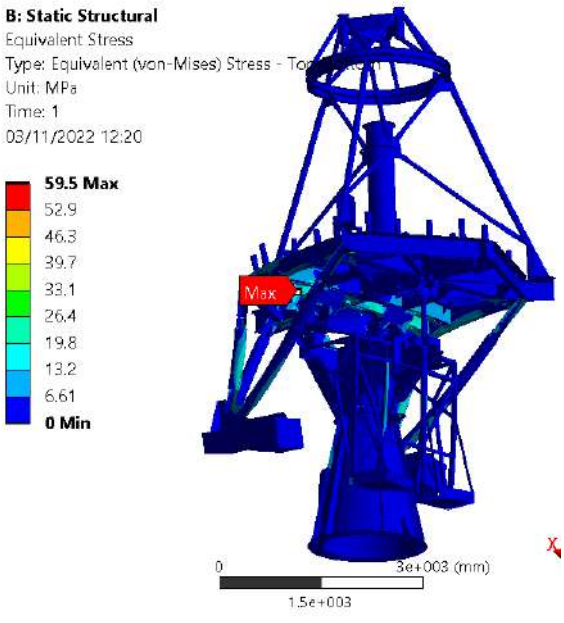

Figure 4-18 – Stress gravity load case (EL 90°) max = 59.5 MPa

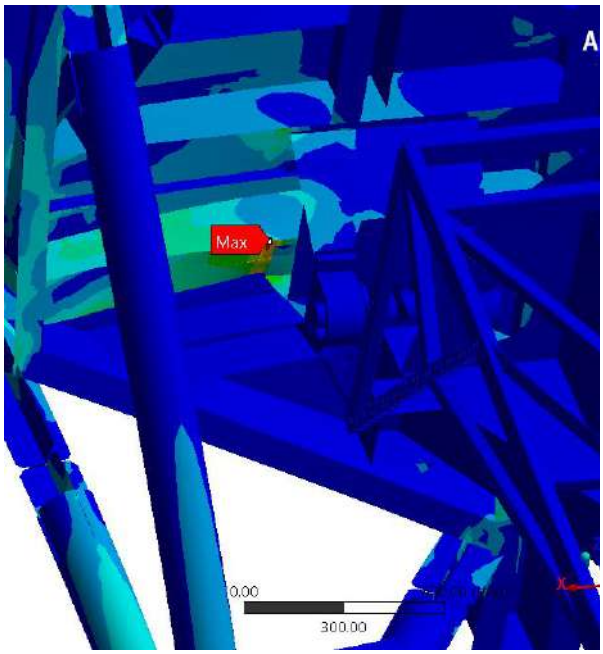

Figure 4-19 – Detail around the maximum stress point (EL 90°)

4.4.1.2 Elevation angle 60°, Gravity (stress)

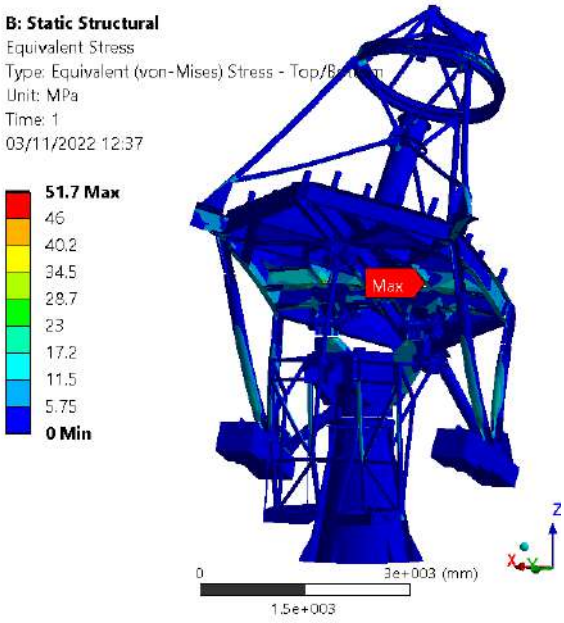

Figure 4-20 – Stress gravity load case (EL 60°) max = 51.7 MPa

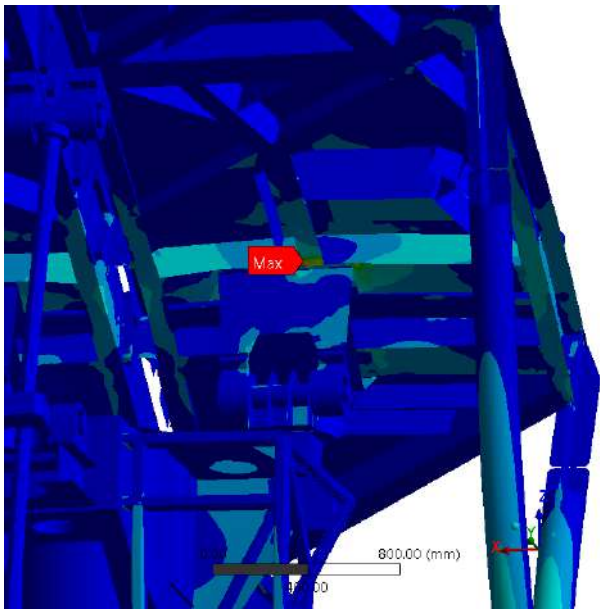

Figure 4-21 – Detail around the maximum stress point (EL 60°)

4.4.1.3 Elevation angle 30°, Gravity (stress)

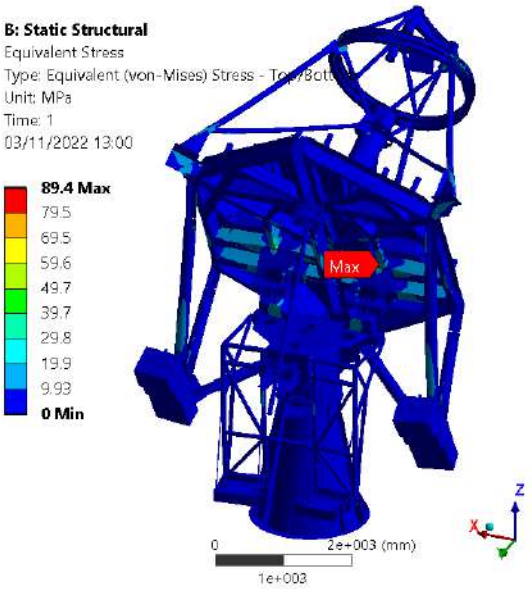

Figure 4-22 – Stress gravity load case (EL 20°) max = 89.4 MPa

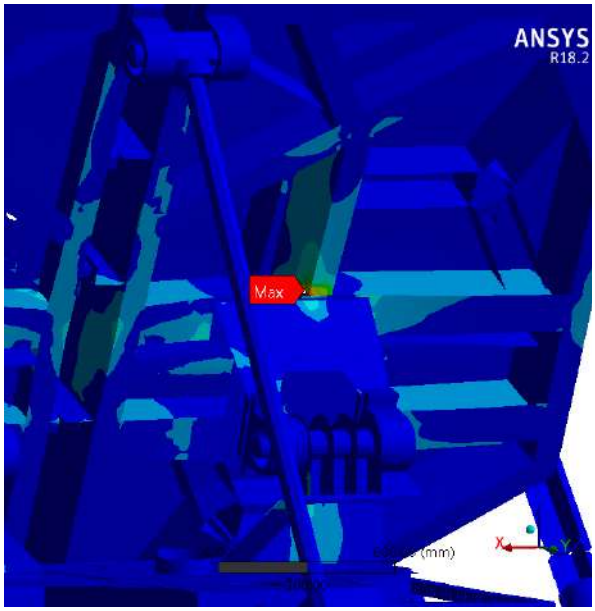

Figure 4-23 – Detail around the maximum stress point (EL 20°)

4.4.1.4 Elevation angle 0°, Gravity (stress)

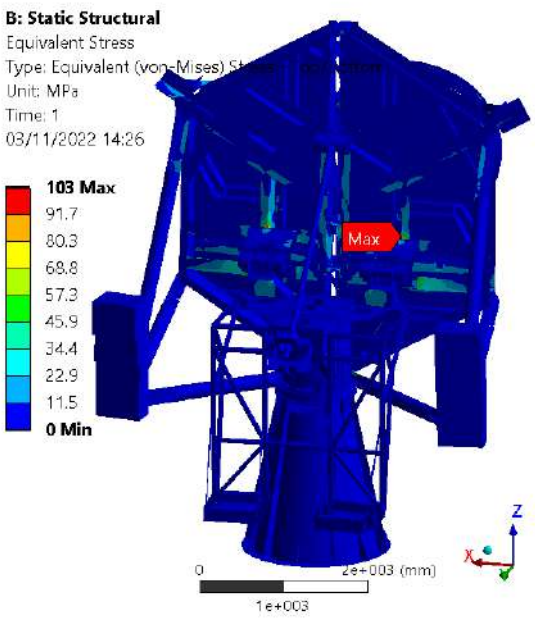

Figure 4-24 – Stress gravity load case (EL 0°) max = 103 MPa

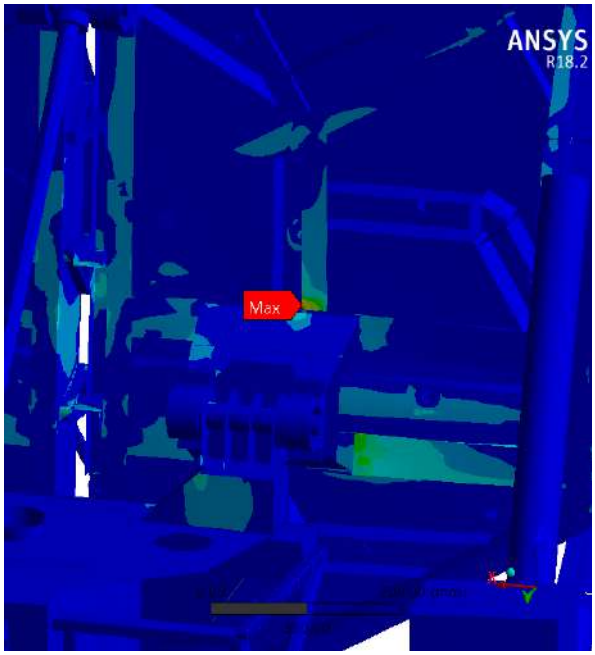

Figure 4-25 – Detail around the maximum stress point (EL 0°)

4.4.2 Static analysis: Deformation

The static analyses results are reported in this section with particular focus on the structure deformation and optics misalignments.

In first are reported the total structural deformations, while tilt, piston and decentering of the optics are shown in a second time.

4.4.2.1 Static analysis: Telescope deformation

As can be seen in the summary table and in the detailed figures of each one of the four cases considered in the analyses below, the maximum total displacement on the whole structure, due to self-weight, is about 2 mm:

Load case	Elevation angle [deg]	Max deformation [mm]	Component
Gravity	90	2.4	Counterweights
	60	1.7	M2 bus
	30	2.8	M2 bus
	0	4.3	M2 bus

Table 19 – Summary of static analyses: Deformation

4.4.2.1.1 Elevation angle 90°, Gravity (deformation)

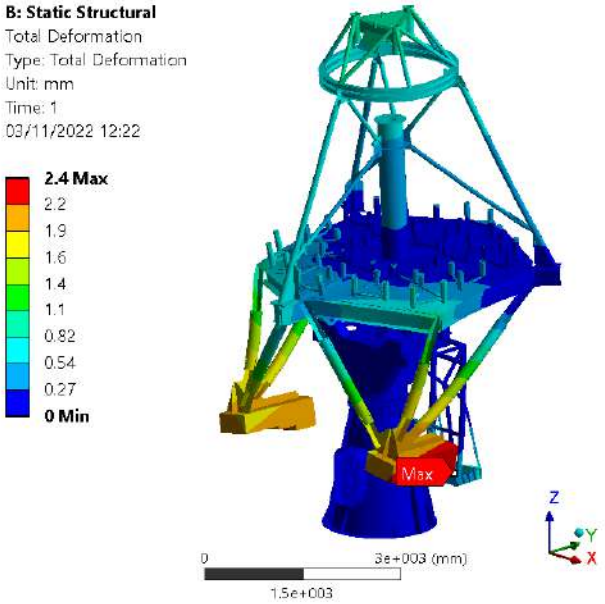

Figure 4-26 – Gravity load case deformation (EL 90°)
Max deformation = 2.4 mm

4.4.2.1.2 Elevation angle 60°, Gravity (deformation)

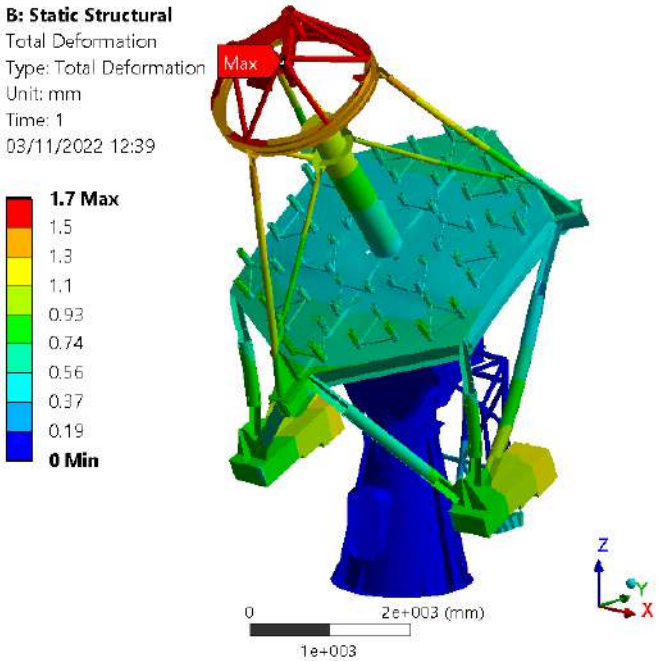

Figure 4-27 – Gravity load case deformation (EL 60°)
Max deformation = 1.7 mm

4.4.2.1.3 Elevation angle 30°, Gravity (deformation)

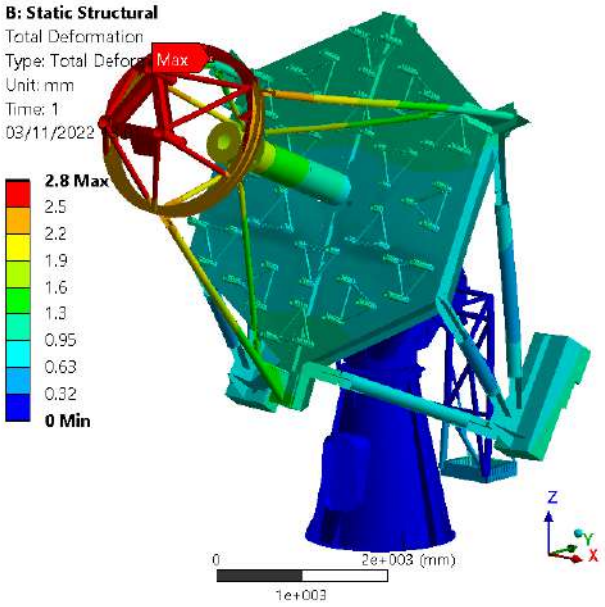

Figure 4-28 – Gravity load case deformation (EL 20°)
Max deformation = 2.8 mm

4.4.2.1.4 Elevation angle 0°, Gravity (deformation)

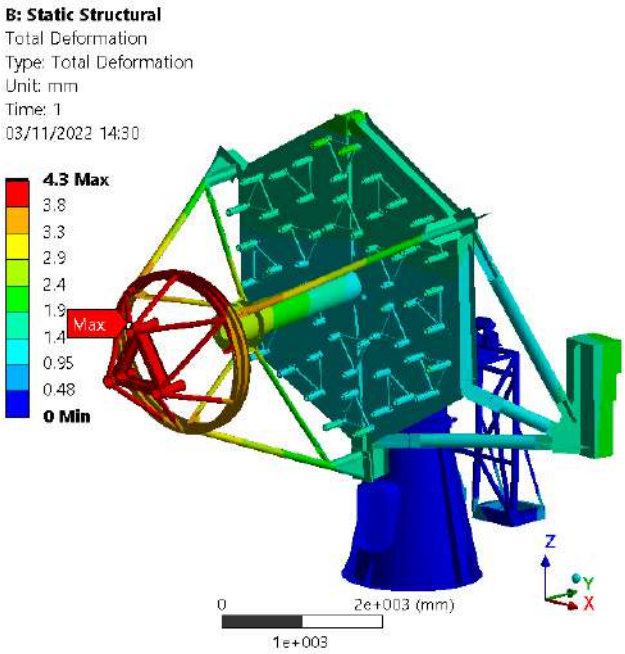

Figure 4-29 – Gravity load case deformation (EL 0°)
Max deformation = 4.3 mm

4.4.2.2 Static analysis: Optics misalignment

The misalignment of the optics and of the camera was evaluated by decomposing the total movements into the following components: Piston, Tilt (Radial and tangential), and Decentering (X and Y). The figure below shows the reference systems used for the calculation of the various components of misalignment and tilt, decomposed into radial and tangential for the segments of M1, and into Tilt X and Tilt Y for the secondary mirror and for the Cherenkov camera.

The 18 mirror segments were divided into 3 groups, based on the distance between the segment and the optical axis. The six inmost mirrors are named with the prefix "i_", the six intermediates with the prefix "m_", and the six outmost segments with the prefix "o_".

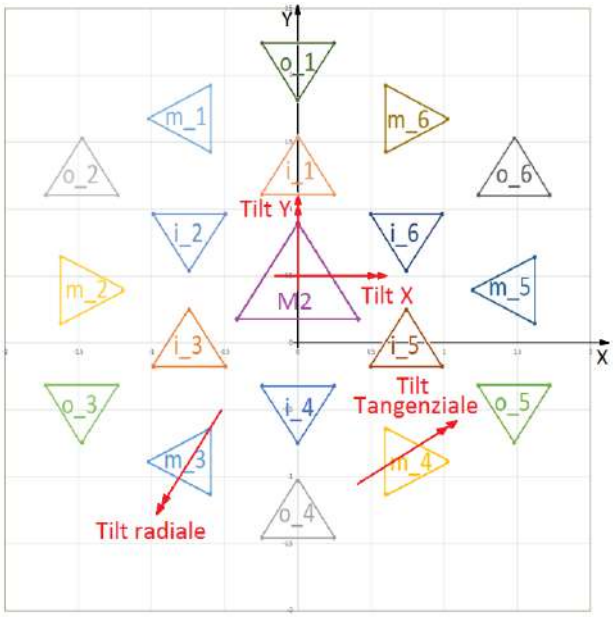

Figure 4-30 – Reference systems for: Tilt, Piston and decentering

The table below shows the Piston values of the individual mirror segments of M1, M2, and camera at three different elevation angles:

Component	Piston (EL 90°) [m]	Piston (EL 20°) [m]	Piston (EL 0°) [m]	Difference 20°-0° [m]	Difference 90°-0° [m]
i_1	9.60E-06	3.10E-04	3.73E-04	-6.22E-05	-3.63E-04
i_2	-4.92E-05	2.71E-04	3.44E-04	-7.22E-05	-3.93E-04
i_3	-1.40E-04	1.70E-04	2.46E-04	-7.65E-05	-3.86E-04
i_4	-1.66E-04	7.21E-06	6.57E-05	-5.85E-05	-2.32E-04
i_5	-1.35E-04	1.40E-04	2.17E-04	-7.69E-05	-3.52E-04
i_6	-4.42E-05	2.47E-04	3.14E-04	-6.77E-05	-3.59E-04
m_1	3.05E-05	3.17E-04	3.85E-04	-6.84E-05	-3.55E-04
m_2	-2.28E-04	2.35E-04	3.69E-04	-1.34E-04	-5.97E-04
m_3	-2.78E-04	-7.71E-05	1.92E-05	-9.63E-05	-2.97E-04
m_4	-2.74E-04	-1.11E-04	-2.43E-05	-8.69E-05	-2.49E-04
m_5	-2.14E-04	1.83E-04	3.05E-04	-1.23E-04	-5.20E-04

Component	Piston (EL 90°) [m]	Piston (EL 20°) [m]	Piston (EL 0°) [m]	Difference 20°-0° [m]	Difference 90°-0° [m]
m_6	3.84E-05	2.95E-04	3.55E-04	-6.01E-05	-3.17E-04
o_1	9.17E-05	3.67E-04	4.25E-04	-5.83E-05	-3.34E-04
o_2	-6.21E-05	2.60E-04	3.51E-04	-9.13E-05	-4.13E-04
o_3	-3.87E-04	1.56E-04	3.31E-04	-1.75E-04	-7.18E-04
o_4	-2.88E-04	-2.44E-04	-1.75E-04	-6.88E-05	-1.13E-04
o_5	-3.76E-04	9.93E-05	2.59E-04	-1.59E-04	-6.35E-04
o_6	-4.75E-05	2.13E-04	2.90E-04	-7.79E-05	-3.38E-04
M2	-1.78E-04	6.04E-05	1.54E-04	-9.33E-05	-3.32E-04
Camera	-7.73E-05	1.77E-04	2.39E-04	-6.12E-05	-3.16E-04

Table 20 – Piston results

The table below shows the tangential Tilt values of the individual mirror segments of M1, M2, and camera at three different elevation angles:

Component	Tangential tilt (EL 90°) [arcsec]	Tangential tilt (EL 20°) [arcsec]	Tangential tilt (EL 0°) [arcsec]	Difference 20°-0° [arcsec]	Difference 90°-0° [arcsec]
i_1	-20.02	-20.19	-19.79	-0.40	-0.23
i_2	0.66	-2.51	-6.57	4.06	7.23
i_3	32.27	0.81	-12.08	12.89	44.35
i_4	30.07	60.26	59.14	1.12	-29.06
i_5	30.23	9.00	-3.56	12.56	33.79
i_6	-0.81	3.29	0.97	2.32	-1.78
m_1	-13.91	-5.15	-5.25	0.10	-8.65
m_2	42.06	2.35	-15.23	17.58	57.29
m_3	52.42	35.11	20.11	15.00	32.31
m_4	51.39	39.12	25.12	14.01	26.27
m_5	40.45	10.08	-6.03	16.11	46.47
m_6	-15.12	-2.01	-1.25	-0.76	-13.87
o_1	-20.08	-10.94	-9.00	-1.94	-11.08
o_2	5.45	6.51	1.29	5.22	4.15
o_3	87.40	5.06	-25.56	30.62	112.96
o_4	29.41	63.72	61.92	1.80	-32.52
o_5	85.14	13.56	-16.96	30.52	102.10
o_6	3.45	12.31	8.77	3.53	-5.33
M2 [Tilt X]	26.20	-16.88	-22.10	5.22	48.31
Camera [Tilt X]	16.45	43.28	45.66	-2.38	-29.21

Table 21 – Tangential tilt and Tilt X results

The table below shows the radial Tilt values of the individual mirror segments of M1, M2, and camera at three different elevation angles:

Component	Radial tilt (EL 90°) [arcsec]	Radial tilt (EL 20°) [arcsec]	Radial tilt (EL 0°) [arcsec]	Difference 20°-0° [arcsec]	Difference 90°-0° [arcsec]
i_1	-0.97	3.14	4.11	-0.97	-5.08
i_2	-19.43	-13.86	-11.11	-2.75	-8.32
i_3	-15.45	-49.11	-53.53	4.42	38.08
i_4	0.27	-3.79	-4.83	1.04	5.10
i_5	16.10	46.69	49.67	-2.97	-33.56
i_6	18.64	17.17	15.49	1.68	3.16
m_1	-17.27	-16.87	-13.86	-3.01	-3.41
m_2	-47.50	-3.54	10.22	-13.75	-57.72
m_3	20.01	-55.33	-71.78	16.45	91.79
m_4	-18.26	48.85	64.50	-15.65	-82.76
m_5	47.82	4.92	-8.93	13.84	56.74
m_6	15.58	22.67	21.04	1.63	-5.46
o_1	-1.07	3.40	3.44	-0.04	-4.51
o_2	-40.78	-10.15	1.23	-11.38	-42.01
o_3	-4.01	-46.60	-53.27	6.67	49.27
o_4	1.26	-5.97	-6.75	0.77	8.01
o_5	4.78	43.93	49.97	-6.04	-45.19
o_6	40.59	14.33	3.48	10.86	37.11
M2 [Tilt Y]	-0.47	4.74	5.43	-0.69	-5.90
Camera [Tilt Y]	-1.05	3.08	3.89	-0.81	-4.95

Table 22 – Radial tilt and Tilt Y results

The table below shows the values of decentering along the Y direction of the individual mirror segments, of M2, and of the camera at three different angles of elevation:

Component	Decentering Y (EL 90°) [m]	Decentering Y (EL 20°) [m]	Decentering Y (EL 0°) [m]
M1	-2.14E-04	-5.25E-04	-4.93E-04
M2	-5.00E-04	-1.70E-03	-1.73E-03
Camera	-4.05E-04	-1.05E-03	-1.04E-03

Table 23 – Y Decentering results

The table below shows the values of decentering along the X direction of the individual mirror segments, of M2, and of the camera at three different angles of elevation:

Component	Decentering X (EL 90°) [m]	Decentering X (EL 20°) [m]	Decentering X (EL 0°) [m]
M1	6.23E-06	1.39E-05	1.59E-05
M2	-1.01E-05	6.48E-05	7.93E-05
Camera	-4.39E-06	4.64E-05	5.69E-05

Table 24 – X Decentering results

4.5 Seismic Analysis Results

The analysis is performed for two different angles of elevation, EL 0° and EL 60°. These angles are those that statistically the telescope most often assumes during its operating life, in particular EL 0° during the non-operation phase (parking position) and EL 60° during the observation phase.

The results shown below refer to analyses carried out with the seismic loads described in the "Collapse prevention" scenario of [AD4], that is the most sever of the two types of events that the structure can be subjected during its operational life. The detail of the load curve and the method of combination in the three directions are described in section 4.2.2.

During the evaluation of the spectrum analysis results, it must be kept in mind that the response spectrum provides the maximum possible stress that the structure can support during the entire seismic event. It is unlikely that all modal maxima act simultaneously and are of the same sign, so in reality the stress will probably be smaller than that resulting from the response spectrum analysis. Therefore, a stress value higher than the elastic limit of the material does not necessarily imply the failure of the component.

4.5.1 Seismic analysis results: EL 60°

In the image below are displayed the stress pattern present in the structure due to seismic load for an elevation angle equal to 60°:

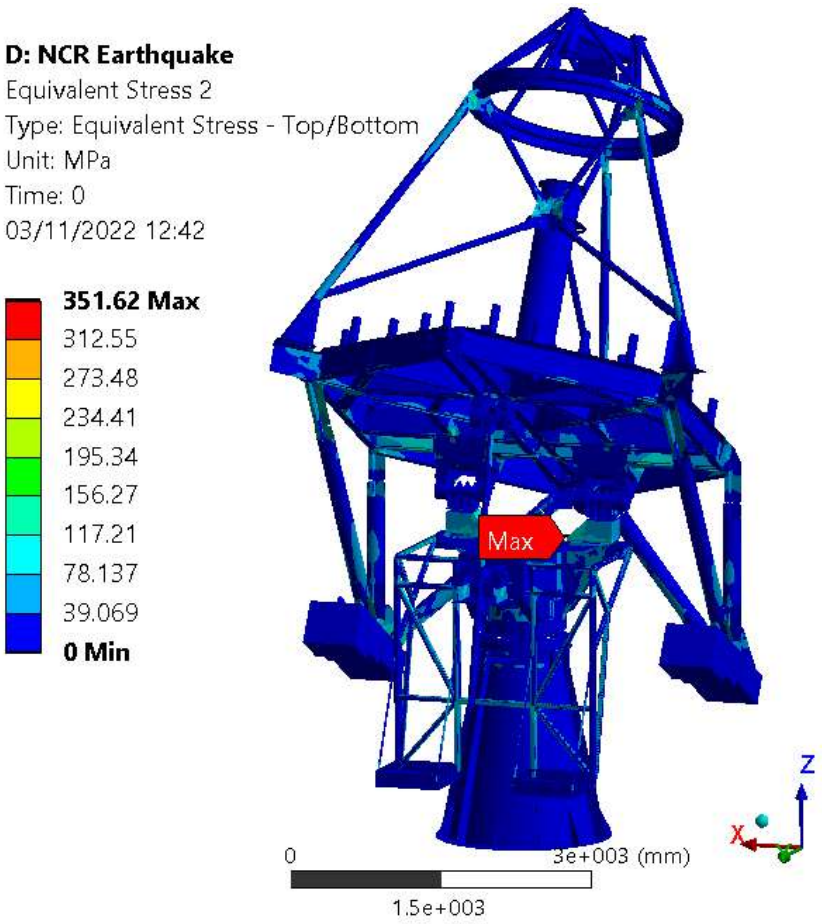

Figure 4-31 – Seismic analysis stress EL 60°

As can be seen, the average stress present in the structure is lower than 100 MPa, with the exception of one very localized peak that exceed 350 MPa, in correspondence with the red arrow-shaped indicator.

4.5.2 Seismic analysis results: EL 0°

In the image below are shows the stress pattern present in the structure due to seismic load for an elevation angle equal to 0°:

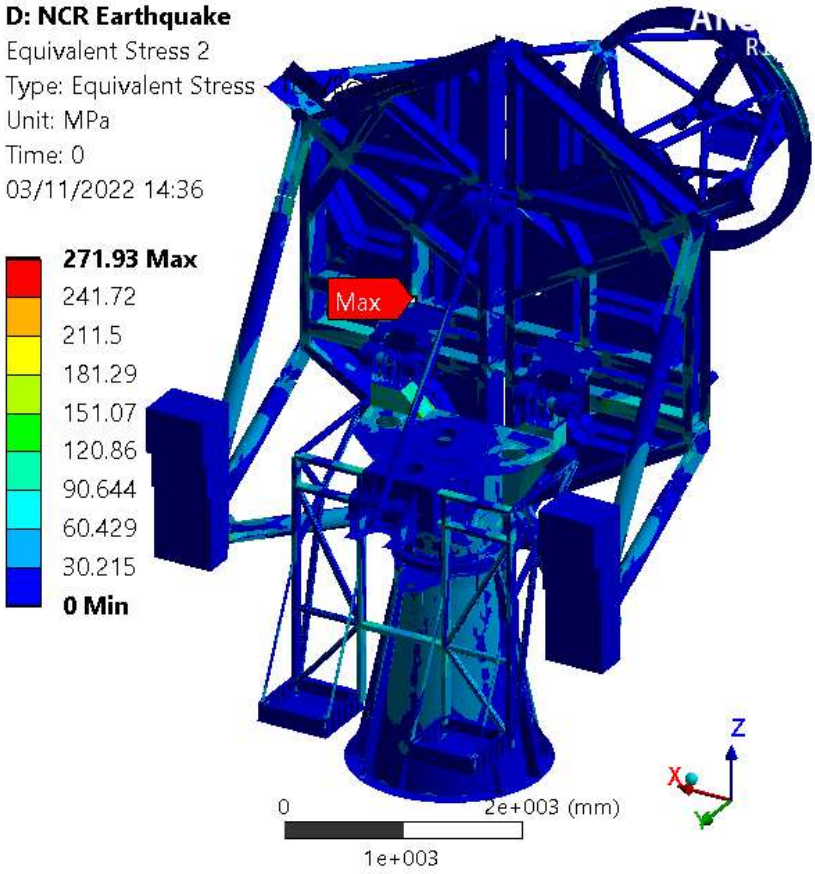

Figure 4-32 – Seismic analysis stress EL 0°

As can be seen in the above figure, the average stress present in the structure is lower than 100 MPa, with the exception of a very localized peak that exceeds 270 MPa, corresponding to the red arrow-shaped indicator.

4.5.3 Buckling verification

For both EL 0° and EL 60° a buckling analysis was performed on a static acceleration which was equal to the peak value for the main frequencies of the system:

- X and Y direction, the peak acceleration value in the band 2.85-10Hz is 21,421 m/s^2
- Z direction, the peak acceleration value in the band 3.33-20 Hz is 16457 m/s^2

These values were used in two static analysis, one with the earthquake acceleration Z going against gravity and one in the same direction of gravity.

4.5.3.1 Results at EL 0°

The first structurally relevant mode happens at EL 0° for a multiplier of 3.87 on the actuator screw.

There are thus no relevant issues on the structure's local instabilities due to earthquakes.

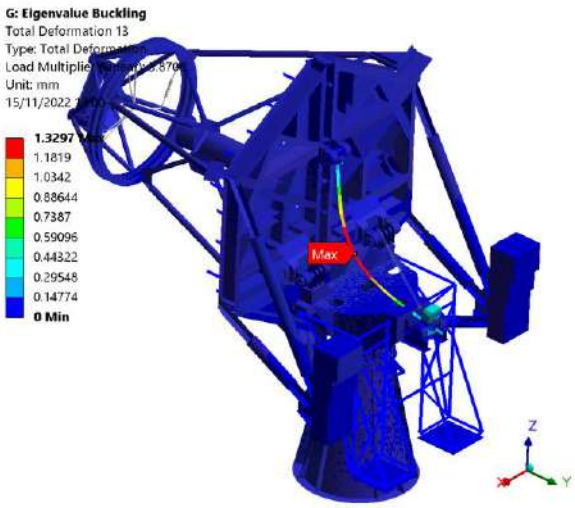

Figure 4-33 – first relevant multiplier (Z acc. downwards), EL 0°

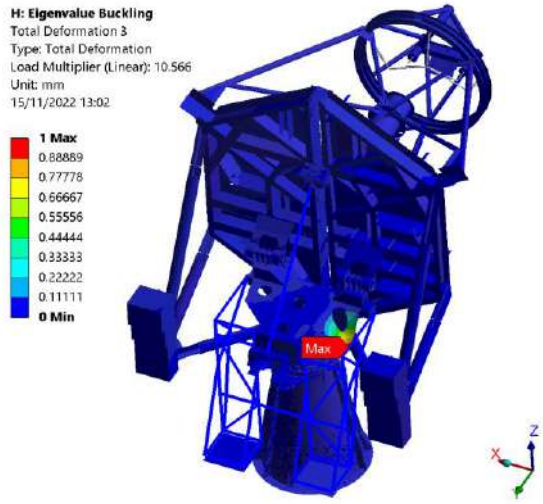

Figure 4-34 – first relevant multiplier (Z acc. upwards), EL 0°

4.5.3.2 Results at EL 60°

For EL 60° there are no structurally relevant modes up to the 50th. Only some instability on the M1 dish main plate occurs (though at multipliers starting from 5.5), which do not compromise structural integrity anyway.

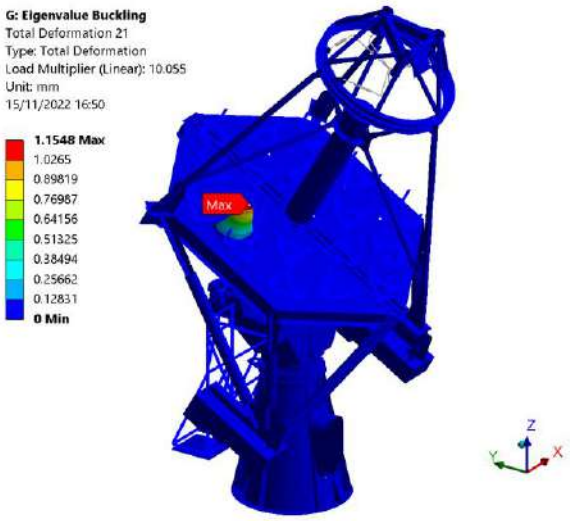

Figure 4-35 – first dish multiplier (Z acc. downwards), EL 0°

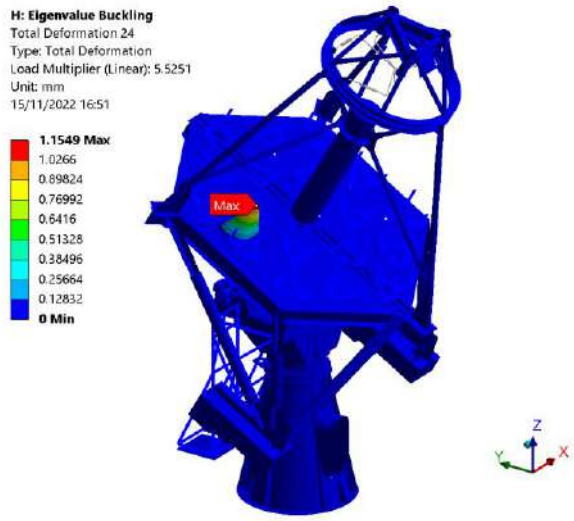

Figure 4-36 – first dish multiplier (Z acc. upwards), EL 0°

5 Conclusions

This document is prepared to present and comment the results of the numerical analyses carried out, in order to verify the static and dynamic behavior of the SST telescope under the external loads defined by the technical specification.

Through the analyses carried out, it is possible to conclude that the proposed structure is able to meet the design requirements and to adequately withstand the external loads. Below there is a summary of the results obtained:

5.1 Modal Analysis

A series of modal analyses were conducted, at different angles of elevation (90°, 60°, 20° 0°), which allowed to describe the dynamic behavior of the structure, and to compare the values of the first frequencies with the limits imposed by the specifications, which requires a first frequency higher than 2.5 Hz (D-SST-MEC-0680 of [RD2]).

The table below summarizes the values of the first 15 frequencies of the telescope for the four elevation angles taken into consideration:

Mode	EL 90°	EL 60°	EL 30°	EL 0°
	Freq [Hz]	Freq [Hz]	Freq [Hz]	Freq [Hz]
1	5.38	5.27	5.08	4.30
2	5.46	5.43	5.40	4.90
3	6.20	6.51	5.81	5.39
4	6.91	6.79	6.35	6.03
5	7.27	6.90	7.20	7.22
6	8.15	7.90	8.03	8.68
7	8.75	8.75	8.75	8.74
8	8.93	8.93	8.94	8.94
9	9.83	9.76	9.68	9.97
10	10.27	10.23	10.30	10.38
11	10.53	12.09	12.09	12.09
12	11.59	12.09	12.09	12.09
13	12.09	12.14	12.14	12.14
14	12.09	12.17	12.17	12.17
15	12.14	12.66	12.65	12.65

Table 25 – Modal analyses summary

As it is possible to see from the data in the table the first telescope frequency is always higher than 2.5 Hz, meeting the specification, for any elevation angles.

The details of the results and analyses are shown in chapter 0.

5.2 Static Analyses

A series of static analyzes were carried out, in order to verify both the internal stress caused by the telescope own weight, and the misalignment of the optical elements due to the deformations of the structure.

The table below summarizes the values of the peaks stress and the related safety factors.

Load case	Elevation angle [deg]	Telescope Structure				
		σVM,max [MPa]	SFy	notes	SFu	notes
Gravity	90	59.5	6.0	C	8.2	C
	60	51.7	6.9	C	9.5	C
	30	89.4*	4.0	C	5.5	C
	0	103*	3.4	C	4.8	C
SF=Additional Safety Factor C=Compliant *punctual stress						

Table 26 – Static analyses summary (stress)

As you can see, all the additional safety factors are much higher than what is usually taken as limit in the structural engineering practice (1.5), verifying that all the components of the telescope remain in the linear elastic behavior. Details of the results and analyses are shown in chapter 4.4.

The misalignments of the optical components and the camera were evaluated by decomposing them into Piston, Tilt, and Decentering. The values of these misalignments are summarized in the following tables. For all the details of the results and analyses carried out, refer to chapter 4.4.2.2

Component	Piston (EL 90°) [m]	Piston (EL 20°) [m]	Piston (EL 0°) [m]	Difference 20°-0° [m]	Difference 90°-0° [m]
M1 RMS	1,99E-04	2,25E-04	2,95E-04	-6,98E-05	-9,65E-05
M2	-1,78E-04	6,04E-05	1,54E-04	-9,33E-05	-3,32E-04
Camera	-7,73E-05	1,77E-04	2,39E-04	-6,12E-05	-3,16E-04

Table 27 – Piston results

Component	Tangential tilt (EL 90°) [arcsec]	Tangential tilt (EL 20°) [arcsec]	Tangential tilt (EL 0°) [arcsec]	Difference 20°-0° [arcsec]	Difference 90°-0° [arcsec]
M1 RMS	39,91	25,41	23,99	1,42	15,92
M2 [Tilt X]	26,20	-16,88	-22,10	5,22	48,31
Camera [Tilt X]	16,45	43,28	45,66	-2,38	-29,21

Table 28 – Tangential tilt results

Component	Radial tilt (EL 90°) [arcsec]	Radial tilt (EL 20°) [arcsec]	Radial tilt (EL 0°) [arcsec]	Difference 20°-0° [arcsec]	Difference 90°-0° [arcsec]
M1 RMS	24,03	29,67	34,38	-4,71	-10,35
M2 [Tilt Y]	-0,47	4,74	5,43	-0,69	-5,90
Camera [Tilt Y]	-1,05	3,08	3,89	-0,81	-4,95

Table 29 – Radial tilt results

Component	Y decentering (EL 90°) [m]	Y decentering (EL 20°) [arcsec]	Y decentering (EL 0°) [arcsec]
M1	-2.14E-04	-5.25E-04	-4.93E-04
M2	-5.00E-04	-1.70E-03	-1.73E-03
Camera	-4.05E-04	-1.05E-03	-1.04E-03

Table 30 – Y decentring results

Component	X decentering (EL 90°) [m]	X decentering (EL 20°) [arcsec]	X decentering (EL 0°) [arcsec]
M1	6.23E-06	1.39E-05	1.59E-05
M2	-1.01E-05	6.48E-05	7.93E-05
Camera	-4.39E-06	4.64E-05	5.69E-05

Table 31 – X decentring results

5.3 Seismic Analysis

Two seismic analyses were carried out to evaluate the structural stress, one for an elevation angle of 60° and one for an elevation angle of 0° (pointing to the horizon). Both referring to the scenario described by the "Collapse prevention" specification [AD4].

As described in chapter 4.5, the stress peaks in the two analyses are lower than the material yield point and no structural instability occurs under the peak combined accelerations.

Thus, no damage to the telescope structure is predicted even in the event of an NCR level earthquake.

End of the document